368–371.
79. Ramis, A., Latimer, K. S., Niagro, F. D., Campagnoli, R. P., Ritchie, B. W. and Pesti, D. 1994. Diagnosis of psittacine beak and feather disease (PBFD) viral infection, avian polyomavirus infection, adenovirus infection and herpesvirus infection in psittacine tissues using DNA in situ hybridization. *Avian Pathol.* **23**: 643–657.
80. Ramis, A., Marlasca, M. J., Majo, N. and Ferrer, L. 1992. Inclusion body hepatitis (IBH) in a group of eclectus parrots (*Eclectus roratus*). *Avian Pathol.* **21**: 165–169.
81. Raue, R., Gerlach, H. and Muller, H. 2005. Phylogenetic analysis of the hexon loop 1 region of an adenovirus from psittacine birds supports the existence of a new psittacine adenovirus (PsAdV). *Arch. Virol.* **150**: 1933–1943.
82. Raue, R., Johne, R., Crosta, L., Burkle, M., Gerlach, H. and Muller, H. 2004. Nucleotide sequence analysis of a C1 gene fragment of psittacine beak and feather disease virus amplified by real-time polymerase chain reaction indicates a possible existence of genotypes. *Avian Pathol.* **33**: 41–50.
83. Ritchie, B. W., Niagro, F. D., Latimer, K. S., Steffens, W. L., Pesti, D. and Lukert, P. D. 1991. Hemagglutination by psittacine beak and feather disease virus and use of hemagglutination inhibition for detection of antibodies against the virus. *Am. J. Vet. Res.* **52**: 1810–1815.
84. Ritchie, B. W., Niagro, F. D.,Lukert, P. D., Steffens, W. D. 3rd. and Latimer, K. S. 1989. Characterization of a new virus from cockatoos with psittacine beak and feather disease. *Virology* **171**: 83–88.
85. Ritchie, B. W., Vaughn, S. B., Leger, J. S., Rich, G. A., Rupiper, D. J., Forgey, G., Greenacre, C. B., Latimer, K. S., Pesti, D., Campagnoli, R. and Lukert, P. D. 1998. Use of an inactivated virus vaccine to control polyomavirus outbreaks in nine flocks of psittacine birds. *J. Am. Vet. Med. Assoc.* **212**: 685–690.
86. Ritchie, P. A., Anderson, I. L. and Lambert, D. M. 2003. Evidence for specificity of psittacine beak and feather disease viruses among avian hosts. *Virology* **306**: 109–115.
87. Roberts, M. M., White, J. L., Grutter, M. G. and Burnett, R. M. 1986. Three-dimensional structure of the adenovirus major coat protein hexon. *Science* **232**: 1148–1151.
88. Rott, O., Kroger, M., Muller, H. and Hobom, G. 1988. The genome of budgerigar fledgling disease virus, an avian polyomavirus. *Virology* **165**: 74–86.
89. Sanada, N. and Sanada, Y. 2007. Epidemiological survey of psittacine beak and feather disease in Japan. (Japanese) *J. Jpn. Vet. Med. Assoc.* **60**: 61–65.
90. Scott, P. C., Condron, R. J. and Reece, R. L. 1986. Inclusion body hepatitis associated with adenovirus-like particles in a cockatiel (*Psittaciformes; Nymphicus hollandicus*). *Aust. Vet. J.* **63**: 337–338.
91. Simpson, C. F. and Hanley, J. E. 1977. Pacheco's parrot disease of psittacine birds. *Avian Dis.* **21**: 209–219.
92. Simpson, C. F., Hanley, J. E. and Gaskin, J. M. 1975. Psittacine herpesvirus infection resembling pacheco's parrot disease. *J. Infect. Dis.* **131**: 390–396.
93. Stanford, M. 2004. Interferon treatment of circovirus infection in grey parrots (*Psittacus erithacus*). *Vet. Rec.* **154**: 435–436.
94. Stoll, R., Hobom, G. and Muller, H. 1994. Host restriction in the productive cycle of avian polyomavirus budgerigar fledgling disease virus type 3 depends on a single amino acid change in the common region of structural proteins VP2/VP3. *J. Gen. Virol.* **75**: 2261–2269.
95. Stoll, R., Luo, D., Kouwenhoven, B., Hobom, G. and Muller, H. 1993. Molecular and biological characteristics of avian polyomaviruses: isolates from different species of birds indicate that avian polyomaviruses form a distinct subgenus within the polyomavirus genus. *J. Gen. Virol.* **74**: 229–237.
96. Styles, D. K., Tomaszewski, E. K., Jaeger, L. A. and Phalen, D. N. 2004. Psittacid herpesviruses associated with mucosal papillomas in neotropical parrots. *Virology* **325**: 24–35.
97. Styles, D. K., Tomaszewski, E. K. and Phalen, D. N. 2005. A novel psittacid herpesvirus found in African grey parrots (*Psittacus erithacus erithacus*). *Avian Pathol.* **34**: 150–154.
98. Sundberg, J. P., Junge, R. E., O'Banion, M. K., Basgall, E. J., Harrison, G., Herron, A. J. and Shivaprasad, H. L. 1986. Cloacal papillomas in psittacines. *Am. J. Vet. Res.* **47**: 928–932.
99. Tachezy, R., Rector, A., Havelkova, M., Wollants, E., Fiten, P., Opdenakker, G., Jenson, B., Sundberg, J. and Van Ranst, M. 2002. Avian papillomaviruses: the parrot Psittacus erithacus papillomavirus (PePV) genome has a unique organization of the early protein region and is phylogenetically related to the chaffinch papillomavirus. *BMC Microbiol.* **2**: 19.
100. Thureen, D. R. and Keeler, C. L. Jr. 2006. Psittacid herpesvirus 1 and infectious laryngotracheitis virus: Comparative genome sequence analysis of two avian alphaherpesviruses. *J. Virol.* **80**: 7863–7872.
101. Todd, D. 2004. Avian circovirus diseases: lessons for the study of PMWS. *Vet. Microbiol.* **98**: 169–174.
102. Tomaszewski, E. K., Kaleta, E. F. and Phalen, D. N. 2003. Molecular phylogeny of the psittacid herpesviruses causing Pacheco's disease: correlation of genotype with phenotypic expression. *J. Virol.* **77**: 11260–11267.
103. Tomaszewski, E. K., Wigle, W. and Phalen, D. N. 2006. Tissue distribution of psittacid herpesviruses in latently infected parrots, repeated sampling of latently infected parrots and prevalence of latency in parrots submitted for necropsy. *J. Vet. Diagn. Invest.* **18**: 536–544.
104. Trinkaus, K., Wenisch, S., Leiser, R., Gravendyck, M. and Kaleta, E. F. 1998. Psittacine beak and feather disease infected cells show a pattern of apoptosis in psittacine skin. *Avian Pathol.* **27**: 555–561.
105. Tsai, S. S., Park, J. H., Hirai, K. and Itakura, C. 1993. Herpesvirus infections in psittacine birds in Japan. *Avian Pathol.* **22**: 141–156.
106. van den Brand, J. M., Manvell, R., Paul, G., Kik, M. J. and Dorrestein, G. M. 2007. Reovirus infections associated with high mortality in psittaciformes in The Netherlands. *Avian Pathol.* **36**: 293–299.
107. Van Doorslaer, K., Sidi, A. O., Zanier, K., Rybin, V., Deryckere, F., Rector, A., Burk, R. D., Lienau, E. K., van Ranst, M. and Trave, G. 2009. Identification of unusual E6 and E7 proteins within avian papillomaviruses: cellular localization, biophysical characterization, and phylogenetic analysis. *J. Virol.* **83**: 8759–8770.
108. Winterfield, R. W. and Reed, W. 1985. Avian pox: infection and immunity with quail, psittacine, fowl, and pigeon pox viruses. *Poult. Sci.* **64**: 65–70.
109. Ypelaar, I., Bassami, M. R., Wilcox, G. E. and Raidal, S. R. 1999. A universal polymerase chain reaction for the detection of psittacine beak and feather disease virus. *Vet. Microbiol.* **68**: 141–148.

NOTE *Virology*

Genetic Analysis of Beak and Feather Disease Virus Derived from a Cockatiel (*Nymphicus hollandicus*) in Japan

Hiroshi KATOH[1)], Kenji OHYA[1)], Kenichiro ISE[2)] and Hideto FUKUSHI[1)]

[1)]*Department of Applied Veterinary Sciences, United Graduate School of Veterinary Sciences, Gifu University, Gifu 501–1193 and* [2)]*Yoshiduka ASM Pet Clinic, Fukuoka 812–0041, Japan*

(Received 18 September 2009/Accepted 13 December 2009/Published online in J-STAGE 25 December 2009)

ABSTRACT. Psittacine beak and feather disease (PBFD), which is caused by beak and feather disease virus (BFDV), has been reported in a wide range of psittacine species, except the cockatiel (*Nymphicus hollandicus*), in which PBFD has rarely been reported. We detected BFDV from a case of PBFD in a cockatiel in the present study. The virus was designated CO-JA. The whole genome sequence of CO-JA had from 86 to 98% homology with BFDVs in psittacine species. CO-JA clustered with isolates derived from other cockatoos in phylogenetic analyses based on two major virus proteins. We concluded that genetic data cannot explain the reason why PBFD is rarely found in the cockatiel.

KEY WORDS: beak and feather disease virus, cockatiel, psittacine beak and feather disease, sequence analysis.

J. Vet. Med. Sci. 72(5): 631–634, 2010

Psittacine beak and feather disease (PBFD) is a lethal disease in psittacine species. Clinical signs of PBFD include chronic, progressive loss of feathers and, in some species, deformities of the beak and claws [7]. Beak and feather disease virus (BFDV), the causative agent of PBFD, belongs to the genus *Circovirus* in the family *Circoviridae* [8]. The BFDV genome is a single-stranded circular DNA of approximately 2 kb that consists of 2 major open reading frames (ORFs), ORF1 and ORF2, encoding the replication-associated protein (Rep) and capsid protein (CP), respectively [1, 5].

PBFD was first described in various species of Australian cockatoos, including sulfur-crested cockatoos, lovebirds, budgerigars and galahs, in 1975 and has since been reported to affect more than 60 psittacine species; it is highly probable that all psittacine species are susceptible [4, 7, 9]. However, BFDV infection has rarely been reported in cockatiels. Here, we report the detection and comparative genomic analyses of a BFDV from PBFD in a cockatiel patient to clarify the reason why PBFD is rarely found in cockatiels.

A 3-year old cockatiel was presented to a veterinary hospital with the complaint of deformities of the feather shaft, dystrophic changes in the primary, secondary, tail and crest feathers and beak abnormality for 2 years (Fig.1). A blood sample was obtained from the bird, and then DNA was extracted from the entire volume (50 μl) using a SepaGene nucleic acid extraction kit (Sanko Junyaku Co., Tokyo, Japan) to detect pathogens, including BFDV, avian polyomavirus, psittacid herpesvirus and psittacine adenovirus with real-time PCR assays as previous described [2].

BFDV DNA was detected; no DNA of any other pathogenic virus was found. The genome sequence of this BFDV isolate, which was designated CO-JA, was amplified by PCR using two pairs of primers (Primer 2/PBFDdupR and PBFDdupF/Primer 4) as described previously (Table 1) [6, 10]. The PCR products were directly sequenced by the primer walking method and assembled as described previously [3]. The primers used for walking were designed from published sequences of BFDV in GenBank (Table 1). The sequence read was submitted to DDBJ (Accession number AB514568). The whole genome sequence of CO-JA was 1,991 nucleotides long. The overall percentage of identity ranged from 86% (isolate LK-VIC) and 98% (isolate BFDV-AUS) in the 26 published nucleotide sequences from the public database (Table 2). Sequences derived from cockatiel BFDVs in the other countries (isolates 05–106 and 05–726) were 95% identical to the sequence of CO-JA.

The predicted sizes of Rep and CP were 289 amino acids and 247 amino acids, respectively. The distances of Rep in the CO-JA sequence and other BFDV sequences varied between 1.1% (isolate BFDV-AUS) and 12.1% (isolate LK-VIC) at the amino acid level. Those of CP varied between 3.7% (isolate BFDV-AUS) and 24.3% (isolate LK-VIC). The deduced amino acid sequence of CO-JA showed 97% and 98% homologies in Rep and 93% and 92% homologies in CP to the sequences of cockatiel BFDV isolates 05–106 and 05–726, respectively. As a result of phylogenetic analysis using the neighbor-joining (NJ) method, UPGMA method, maximum parsimony analysis and maximum likelihood approach, the BFDV sequences could be allocated into 11 groups for CP or 10 groups for Rep on the basis of the criteria of >5% divergence, respectively, and the CO-JA sequence clustered with BFDVs isolated from cockatiels and cockatoos (Fig. 2).

Our genetic analyses show that CO-JA is highly similar to other BFDV isolates derived from psittacine species classified into *Psittacinae*. In addition, the clinical symptoms of this bird were similar to those of other psittacine species,

* CORRESPONDENCE TO: FUKUSHI, H., Laboratory of Veterinary Microbiology, Faculty of Applied Biological Sciences, Gifu University, 1–1 Yanagido, Gifu 501–1193, Japan.
e-mail: hfukushi@gifu-u.ac.jp

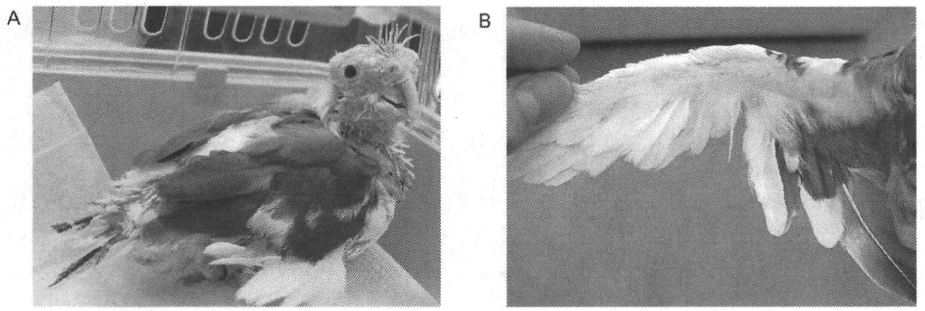

Fig.1. Appearance of this case. (A) The bird showed loss of flight, crest and tail feathers. (B) It also showed abnormality of the primary and secondary flight feathers.

Table 1. DNA sequences of primers used in this study

Primer	Sequence (5'–3')	Position	Reference
Primer 2	AACCCTACAGACGGCGAG	182–199	[10]
Primer 4	GTCACAGTCCTCCTTGTACC	879–898	
PBFDdupF	TTGGGTCCTCCTTGTAGTGGGATC	1371–1394	[6]
PBFDdupR	CAGACGCCGTTTCTCAACCAATAG	1842–1865	
BFDVseq1F	GGTGGCTACCTTATTGCGAG	750–769	This study
BFDVseq2F	TCCTCGCTCACCCCATCAAT	975–994	
BFDVseq3F	GCCAACACTGGTGGTTTGTTT	1775–1795	
BFDVseq4F	CGGGCATATCTTCGTCTAAT	1920–1939	
BFDVseq1R	CCGTCTGTAGGGTTGTTAAG	176–195	
BFDVseq2R	GAAAGTAGCCTTGCAAATGG	280–299	
BFDVseq3R	CCCTAACAATCCCAGCACTT	1237–1256	
BFDVseq4R	GGGATTCAAACGCCTCCTCA	1486–1499	

The position for the primers is that of the BFDV-AUS sequence (AF080560).

Table 2. Reference sequences of BFDV used in this study

Isolate	Host bird	Origin	Accession no.
05–106	Cockatiel (*Nymphicus hollandicus*)	Australia	EF457974
05–726	Cockatiel (*Nymphicus hollandicus*)	Australia	EF457975
BB-WA	Blue bonnet (*Psephotus haematonotus*)	Australia	AF311295
LB-WA	Peach-faced lovebird (*Agapornis roseicollis*)	Australia	AF311296
ELBC-SA	Long-billed corella (*Cacatua tenuirostris*)	Australia	AF311297
Galah-WA	Galah (*Eolophus roseicapillus*)	Australia	AF311298
LK-VIC	Rainbow Lorikeet (*Trichoglossus haematodus*)	Australia	AF311299
MMC-WA	Leadbeater's cockatoo (*Cacatua leadbeateri*)	Australia	AF311300
SCC-NT	Greater sulfur-crested cockatoo (*Cacatua galerita*)	Australia	AF311301
SCC1-WA	Greater sulfur-crested cockatoo (*Cacatua galerita*)	Australia	AF311302
BFDV-AUS	Greater sulfur-crested cockatoo (*Cacatua galerita*)	Australia	AF080560
WBC1-ZA	White-bellied caique (*Pionites leucogaster*)	South Africa	AY450434
UC1-ZA	Umbrella cockatoo (*Cacatua alba*)	South Africa	AY450436
CPA8-ZA	Brown-necked parrot (*Poicephalus robustus*)	South Africa	AY450437
CPA7-ZA	Brown-necked parrot (*Poicephalus robustus*)	South Africa	AY450438
RP1-ZA	Ruppell's parrot (*Poicephalus rueppellii*)	South Africa	AY450439
ARB4-ZA	Red-bellied parrot (*Poicephalus rufiventris*)	South Africa	AY450440
GJP1-ZA	Red-fronted parrot (*Poicephalus gulielmi*)	South Africa	AY450441
BCL1-ZAM	Black-cheeked lovebird (*Agapornis nigrigenis*)	Zambia	AY450442
AFG3-ZA	African grey parrot (*Psittacus erithacus*)	South Africa	AY450443
PK1-01TX	Ring-necked parakeet (*Psittacula krameri*)	U.S.A.	AY521234
AR02-1UK	Peach-faced lovebird (*Agapornis roseicollis*)	United Kingdom	AY521235
PEP01-1POR	African grey parrot (*Psittacus erithacus*)	Portugal	AY521236
PEG07-1GE	African grey parrot (*Psittacus erithacus*)	Germany	AY521237
PEU01-1UK	African grey parrot (*Psittacus erithacus*)	United Kingdom	AY521238
BFDV-USA	Unknown (pooled virus)	U.S.A.	AF071878

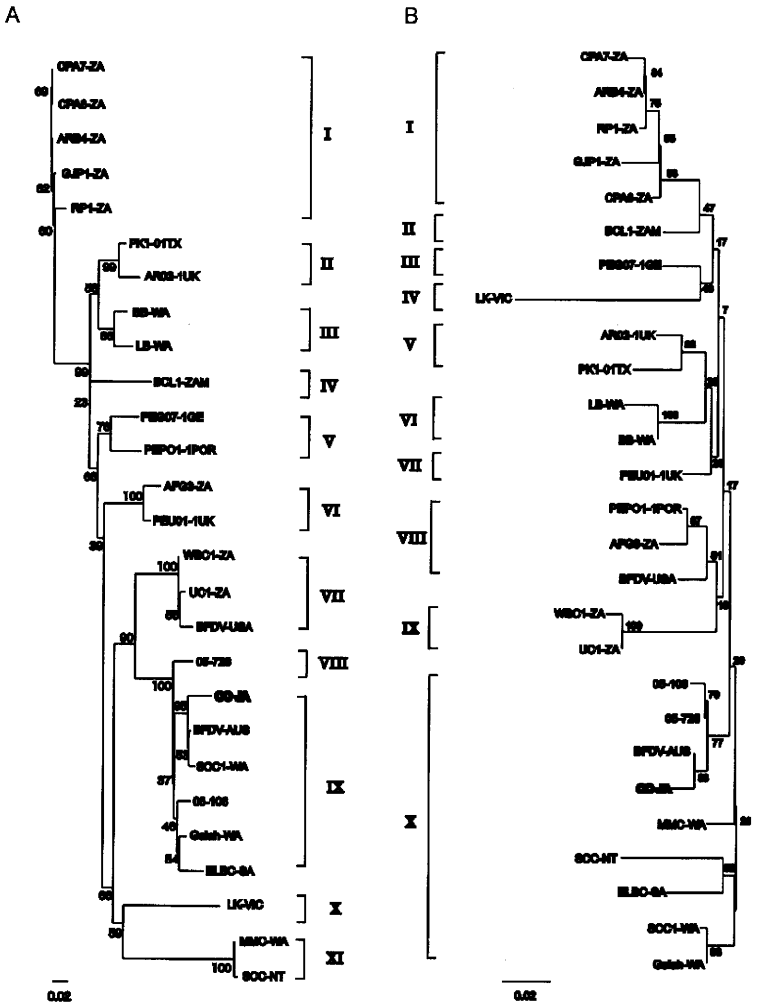

Fig. 2. Bootstrapped phylogenetic trees obtained using the neighbor-joining method based on the nucleotide sequences of CP (A) and Rep (B). The numbers at the nodes indicate the bootstrap values. The scale bars indicate the predicted amino acid substitutions in sites.

including cockatiels, as described previously [8, 10]. The origin of CO-JA and other BFDVs isolated in cockatiels might be identical to the BFDVs in cockatoos, which are classified into the pacific species as well as the cockatiel. Worldwide trade of these pacific bird species could cause spread of these related BFDVs to many countries. It is difficult to explain the cause of the rarity of PBFD in the cockatiel from a genetic point of view. Although no serological approaches were attempted in this study, Shearer *et al.* reported that the BFDVs from cockatiels are serologically different from other BFDVs [9]. In addition, other factors, including the host immune system, could be related to the rare incidence. In conclusion, it is necessary to focus on not only the viral factors but also the host immune system in order to understand BFDV infection in cockatiels.

REFERENCES

1. Bassami, M. R., Berryman, D., Wilcox, G. E. and Raidal, S. R. 1998. Psittacine beak and feather disease virus nucleotide sequence analysis and its relationship to porcine circovirus, plant circoviruses, and chicken anaemia virus. *Virology* **249**: 453–459.
2. Katoh, H., Ohya, K. and Fukushi, H. 2008. Development of novel real-time PCR assays for detecting DNA virus infections in psittaciform birds. *J. Virol. Methods* **154**: 92–98.
3. Katoh, H., Ohya, K., Une, Y., Yamaguchi, T. and Fukushi, H. 2009. Molecular characterization of avian polyomavirus isolated from psittacine birds based on the whole genome sequence analysis. *Vet. Microbiol.* **138**: 69–77.
4. Khalesi, B., Bonne, N., Stewart, M., Sharp, M. and Raidal, S. R. 2005. A comparison of haemagglutination, haemagglutination inhibition and PCR for the detection of psittacine beak and

feather disease virus infection and a comparison of isolates obtained from loriids. *J. Gen. Virol.* **86**: 3039–3046.
5. Niagro, F. D., Forsthoefel, A. N., Lawther, R. P., Kamalanathan, L., Ritchie, B. W., Latimer, K. S. and Lukert, P. D. 1998. Beak and feather disease virus and porcine circovirus genomes: intermediates between the geminiviruses and plant circoviruses. *Arch. Virol.* **143**: 1723–1744.
6. Ogawa, H., Yamaguchi, T. and Fukushi, H. 2005. Duplex shuttle PCR for differential diagnosis of budgerigar fledgling disease and psittacine beak and feather disease. *Microbiol. Immunol.* **49**: 227–237.
7. Pass, D. A. and Perry, R. A. 1984. The pathology of psittacine beak and feather disease. *Aust. Vet. J.* **61**: 69–74.
8. Ritchie, B. W., Niagro, F. D., Lukert, P. D., Steffens, W. L., 3rd and Latimer, K. S. 1989. Characterization of a new virus from cockatoos with psittacine beak and feather disease. *Virology* **171**: 83–88.
9. Shearer, P. L., Bonne, N., Clark, P., Sharp, M. and Raidal, S. R. 2008. Beak and feather disease virus infection in cockatiels (Nymphicus hollandicus). *Avian Pathol.* **37** :75–81.
10. Ypelaar, I., Bassami, M. R., Wilcox, G. E. and Raidal, S. R. 1999. A universal polymerase chain reaction for the detection of psittacine beak and feather disease virus. *Vet. Microbiol.* **68**: 141–148.

Virology 400 (2010) 259–270

Contents lists available at ScienceDirect

Virology

journal homepage: www.elsevier.com/locate/yviro

The ORF37 (UL24) is a neuropathogenicity determinant of equine herpesvirus 1 (EHV-1) in the mouse encephalitis model

Samy Kasem [a], Mi Htay Htay Yu [a], Souichi Yamada [a], Akari Kodaira [b], Tomio Matsumura [c], Koji Tsujimura [c], Hanafy Madbouly [a], Tsuyoshi Yamaguchi [d], Kenji Ohya [b], Hideto Fukushi [a,b,*]

[a] Department of Applied Veterinary Sciences, United Graduate School of Veterinary Sciences, Gifu University, 1-1 Yanagido, Gifu 501-1193, Japan
[b] Laboratory of Veterinary Microbiology, Faculty of Applied Biological Sciences, Gifu University, 1-1 Yanagido, Gifu 501-1193, Japan
[c] Molecular Biology Division, Epizootic Research Center, Equine Research Institute, Japan Racing Association, Shimotsuke, Tochigi 329-0412, Japan
[d] The Avian Zoonosis Research Center, Faculty of Agriculture, Tottori University, 4-101 Koyama Minami, Tottori 680-8550, Japan

ARTICLE INFO

Article history:
Received 28 September 2009
Returned to author for revision
21 January 2010
Accepted 5 February 2010
Available online 2 March 2010

Keywords:
EHV-1
Neuropathogenicity
BAC
UL24
ORF37

ABSTRACT

Equine herpesvirus 1 (EHV-1) bacterial artificial chromosome clone (Ab4p BAC) was established based on neuropathogenic strain Ab4p. ORF37 encoding UL24 was replaced with a selection cassette, rpsL-neo gene, to produce an ORF37 deletion mutant, Ab4pΔORF37. Transfection of RK-13 cells with Ab4pΔORF37 genome DNA produced infectious virus, indicating that ORF37 is not essential for EHV-1 replication in cell culture. Deletion of ORF37 had no effect on the transcript expression of neighboring genes, ORF36 and ORF38, and the growth activity in MDBK cells. Ab4pΔORF37 lost neuropathogenicity in CBA/N1 mice as indicated by the absence of any neurological disorders and death. The growth of Ab4pΔORF37 in cultivated neural cells was one order of magnitude lower than that of parental and revertant viruses. These results indicated that the ORF37 is a neuropathogenicity determinant of EHV-1 in the mouse encephalitis model.

Introduction

Equine herpesvirus 1 (EHV-1) causes respiratory disease, abortion and neurological disorders in the horse (Allen and Bryans, 1986). In recent years, there have been increasing reports of EHV-1-related neurological disorders (Equine herpesvirus myeloencephalopathy, EHM) in the horse in Europe and the United States (Borchers et al., 2006). The neurological symptoms occur in various degrees from mild ataxia to paraplegia. The neurological signs may be caused by vasculitis followed by hemorrhage, thrombosis, hypoxia and secondary ischemic degeneration (Jackson et al., 1977; Kohn and Fenner, 1987).

Characterization of neuropathogenic EHV-1 has begun in recent years at the molecular level. Allen et al. (1983) described 16 electropherotypes, which showed significant differences in DNA fingerprints of EHV-1. The main electropherotypes are P and B, both of which are found in the horse population in Japan (Kirisawa et al., 1993; Matsumura et al., 1992). EHV-1s which were isolated from horses with neurological disorders have been typed EHV-1 P only. EHM caused by EHV-1 B has never been reported so far. Therefore EHV-1 B seems to lose neuropathogenicity in the horse. We previously found that EHV-1 P and B in Japan mainly differed in ORF64, which encodes the immediate early (IE) or the infected cell protein 4 (ICP4) (Pagamjav et al., 2005). We also found that ORF64 of EHV-1 B might be caused by natural recombination between EHV-1 P and EHV-4, another equine pathogen with mild respiratory pathogenicity. Therefore we suggested that ICP4 is possibly involved in the neuropathogenicity of EHV-1. Recent studies have identified a single nucleotide polymorphism (SNP) significantly associated with EHM (Nugent et al., 2006). The SNP is a substitution of adenine (A) by guanine (G), at the nucleotide (nt) 2254 of the EHV-1 gene (ORF30) encoding the viral DNA polymerase and the consequent substitution of asparagine (N) by aspartic acid (D) at amino acid position 752. This hypothesis was supported by later studies based on experimental infection with various field isolates and molecular recombinants (Leutenegger et al., 2008; Yamada et al., 2008; Vissani et al., 2009; Smith et al., 2010). Matsumura et al. (1998) reported that the glycoprotein I (gI, ORF73) and glycoprotein E (gE, ORF74) were

Abbreviations: BAC, bacterial artificial chromosome; bp, base pair; cDNA, complementary deoxyribonucleic acid; DNA, deoxyribonucleic acid; EHV-1, equine herpesvirus type 1; FBS, fetal bovine serum; FEK, fetal equine kidney; GFP, green fluorescent protein; gp2, glycoprotein 2; ICP4, infected cell protein; MDBK, Madin–Darby bovine kidney; MEM, minimum essential medium; MOI, multiplicity of infection; NIH, National Institutes of Health; nt, nucleotide; ORF, open reading frame; PCR, polymerase chain reaction; pfu, plaque-forming unit; RK-13, Rabbit kidney 13; RNA, ribonucleic acid; RT-PCR, reverse transcription and polymerase chain reaction; SPF, specific pathogen free; SV40, simian virus 40; VZV, varicella zoster virus.

* Corresponding author. Laboratory of Veterinary Microbiology, Faculty of Applied Biological Sciences, Gifu University, 1-1 Yanagido, Gifu 501-1193, Japan. Fax: +81 58 293 2946.
E-mail address: hfukushi@gifu-u.ac.jp (H. Fukushi).

0042-6822/$ – see front matter © 2010 Elsevier Inc. All rights reserved.
doi:10.1016/j.virol.2010.02.012

associated with virulence of EHV-1. Thus, multiple genes might be associated with the occurrence of EHM.

The genes of herpesvirus are classified as essential or nonessential for growth in cultured cells; for example, ICP4 and ORF30 are essential genes of EHV-1, while gI and gE are nonessential. Analysis of essential genes is difficult and time consuming with traditional methods that use the homologous recombination in eukaryotic cells which constitutively express the target essential gene product. An alternative approach using bacterial artificial chromosome (BAC) has recently become the preferred method (Brune et al., 2000). This approach allows rapid and efficient alteration of herpes viral genome in *Escherichia coli*. In principle, any essential and non-essential genes on BAC can be modified for deletion, alternation, and replacement with other genes. By establishing a BAC system, researchers can easily perform recombination of any genes including essential and nonessential genes using genetics of *E. coli* (Smith et al., 2005).

Until today, herpesvirus genomes have been cloned as BAC including pseudorabies virus (Smith and Enquist, 2000), human cytomegalovirus (Yu et al., 2002), herpes simplex virus type 1 (Tanaka et al., 2003), varicella zoster virus (Brune et al., 2000), Epstein–Barr virus (Kanda et al., 2004), rhesus cytomegarovirus (Chang and Barry, 2003) and EHV-1 (Goodman et al., 2007; Hansen et al., 2006; Rudolph et al., 2002). Osterrieder and his colleagues have cloned the EHV-1 genome using the KyA, RacL11 and Ab4p strains (Goodman et al., 2007; Rudolph et al., 2002) and Hansen et al. (2006) used the HVS25A strain as sources of BAC. KyA, RacL11 and Ab4p BAC were constructed by insertion of BAC vector sequences into the ORF71 (gp2 gene) in the viral genome. Although the ORF71 is a nonessential gene, its product, gp2, seems to contribute in EHV-1 virulence and pathogenesis (Smith et al., 2005). Therefore, BAC sequences need to be reverted to the original sequences to use these BACs prior to pathogenicity evaluation (Goodman et al., 2007). The HVS25A strain BAC, which had a BAC vector inserted to the intergenic region between ORF62 and ORF63, appeared to have a similar growth to wild-type in cell culture (Hansen et al., 2006). HVS25A strain was isolated from an aborted foal (Whalley et al., 1981) and used in a murine model of respiratory disease (Csellner et al., 1998). However, there is no data about the neuropathogenicity on HVS25A strain. The Ab4p strain is a neurovirulent strain that was isolated from a case of equine paresis (Gibson et al., 1992). Adding with a whole genome sequence (Telford et al., 1992), Ab4p has been confirmed to cause neurological disorders in experimental infection of mice, hamsters and horses (Awan et al., 1990; Fukushi, et al., 2000; Gibson et al., 1992). Therefore Ab4p appears to be the suitable strain for analysis of neuropathogenicity of EHV-1.

EHV-1 UL24 is encoded by ORF37. UL24 homologs are present throughout the Herpesviridae family. The HSV-1 UL24 is a 30-kDa nuclear-associated protein that is not required for growth in cultured cells (Pearson and Coen, 2002). The UL24 homolog identified in bovine herpes virus type 1 (BHV-1) was shown to have a transcription profile similar to that of HSV-1 UL24. Deletion of the BHV-1 UL24 open reading frame (ORF) had little effect on viral replication *in vitro* (Whitbeck et al., 1994). Although the molecular function of UL24 protein is not known, mutation of the HSV-1 gene results in the development of a syncytial plaque-forming phenotype following infection of certain cell types *in vitro*. Studies using HSV-1 UL24 point mutants in a murine ocular disease model suggested that the HSV-1 UL24 gene product was important for peripheral replication in corneal tissue, acute replication in sensory ganglia, and reactivation from explanted mouse ganglia. The UL24 of HSV-2 is reported as a pathogenicity determinant in murine and guinea pig disease models (Blakeney et al., 2005). Inoculating three different types of cell lines with UL24 mutant HSV-2, they reported that it had no effect on viral replication or virus titers as it yielded a cytopathic effect with syncytial formation and virus titers as those produced by the wild-type virus. However, the function of EHV-1 UL24 has not been resolved yet.

In this study, we describe the construction of an infectious BAC of neuropathogenic EHV-1 based on the Ab4p strain (Ab4p BAC). In Ab4p BAC, a BAC vector is inserted into the intergenic region between ORF2 and ORF3. Insertion of a BAC vector into EHV-1 genome was examined by using lambda site-specific recombination technique (Groth and Calos, 2004; Nash, 1990; Nash and Robertson, 1981; Patsey and Bruist, 1995). The BAC sequence could be efficiently removed from the viral genome by using a lambda recombination system, resulting in Ab4p strain without BAC sequence (Ab4p attB). The Ab4p attB showed neurological symptoms in mice and its growth kinetics in cultured cells was the same as that of the wild-type Ab4p. This Ab4p BAC and Ab4p attB will be significant tools for the analyzing the neuropathogenesis of EHV-1. Using this Ab4p BAC, an ORF37 deletion mutation and the corresponding revertant virus were constructed to characterize the ability of the virus to replicate in different cell lines *in vitro* and cause a disease after intranasal inoculation in the CBA/N1 mice model. Our results suggested that the ORF37 has a role in neuropathogenicity of EHV-1 in the mouse model.

Results

Construction of Ab4p BAC and Ab4p attB

We have cloned the full-length EHV-1 Ab4p genome in pZC320-GFP, the modified pZC320 vector, as pAb4p BAC (Fig. 1). We confirmed that pAb4p BAC was maintained in *E. coli*. Ab4p attB was generated by excising the pZC320-GFP sequence from pAb4p BAC by LR clonase reaction and subsequent transfection in RK-13 cells. The NotI digestion sites of the insertion region of pZC320-GFP are shown in Fig. 2A. The digestion of Ab4p BAC genome caused unique 1.4, 5.0 and 5.9 kbp fragments due to the pZC320-GFP insertion (Fig. 2B, lanes 1 and 2). On the other hand, Ab4p and Ab4p attB genome had a 3.1 kbp fragment but not 1.4, 5.0 and 5.9 kb fragments (Fig. 2B lanes 3 and 4). For Ab4p BAC, insertion of pZC320-GFP was confirmed by hybridization to the 1.4 kb fragment with GFP probe (Fig. 2C a, lanes 1 and 2) and the 5.0 kb fragment with ORF3 probe (Fig. 2C b, lanes 1 and 2). For Ab4p attB, excision of pZC320-GFP was confirmed by hybridization to the 3.1 kb fragment with ORF3 probe (Fig. 2C b, lane 3) and no bands with GFP probe (Fig. 2C a, lane 3) as well as Ab4p (Fig. 2C a and b, lane 4).

In vitro growth kinetics and properties of Ab4p BAC and Ab4p attB

Growth properties including the multi-step growth curves and plaque sizes in MDBK cells were compared among Ab4p BAC, Ab4p attB and Ab4p. In multi-step growth kinetics, the growth patterns and final growth titers of Ab4p BAC and Ab4p attB were similar to that of wild-type Ab4p (Fig. 3A). Plaque morphology and average plaque size of Ab4p attB and Ab4p BAC were identical to that of Ab4p (Fig. 3B). There was no significant difference in plaque size among the viruses ($p<0.01$). Therefore, the growth properties of Ab4p BAC and Ab4p attB were concluded to be similar to that of wild-type Ab4p.

Pathogenicity of the Ab4p BAC and Ab4p attB in animal models

The pathogenicity of the Ab4p BAC, Ab4p attB and wild-type Ab4p were evaluated in the mouse model. CBA/N1 mice were inoculated with the viruses intranasally. The body weight and clinical signs were monitored every day for two weeks. The body weight change of Ab4p attB was similar to that of Ab4p. On the other hand, the body weight change of Ab4p BAC was the same as that of control mice. The mice, which were inoculated Ab4p or Ab4p attB virus, showed the same clinical symptoms, such as hyperactivity, paralysis, arching of the back and lethargy. On the other hand, Ab4p BAC showed hyperactivity only after 7 days post inoculation (data not shown).

This result suggested that Ab4p attB maintained the pathogenicity of the wild-type Ab4p but Ab4p BAC lost its pathogenicity in the

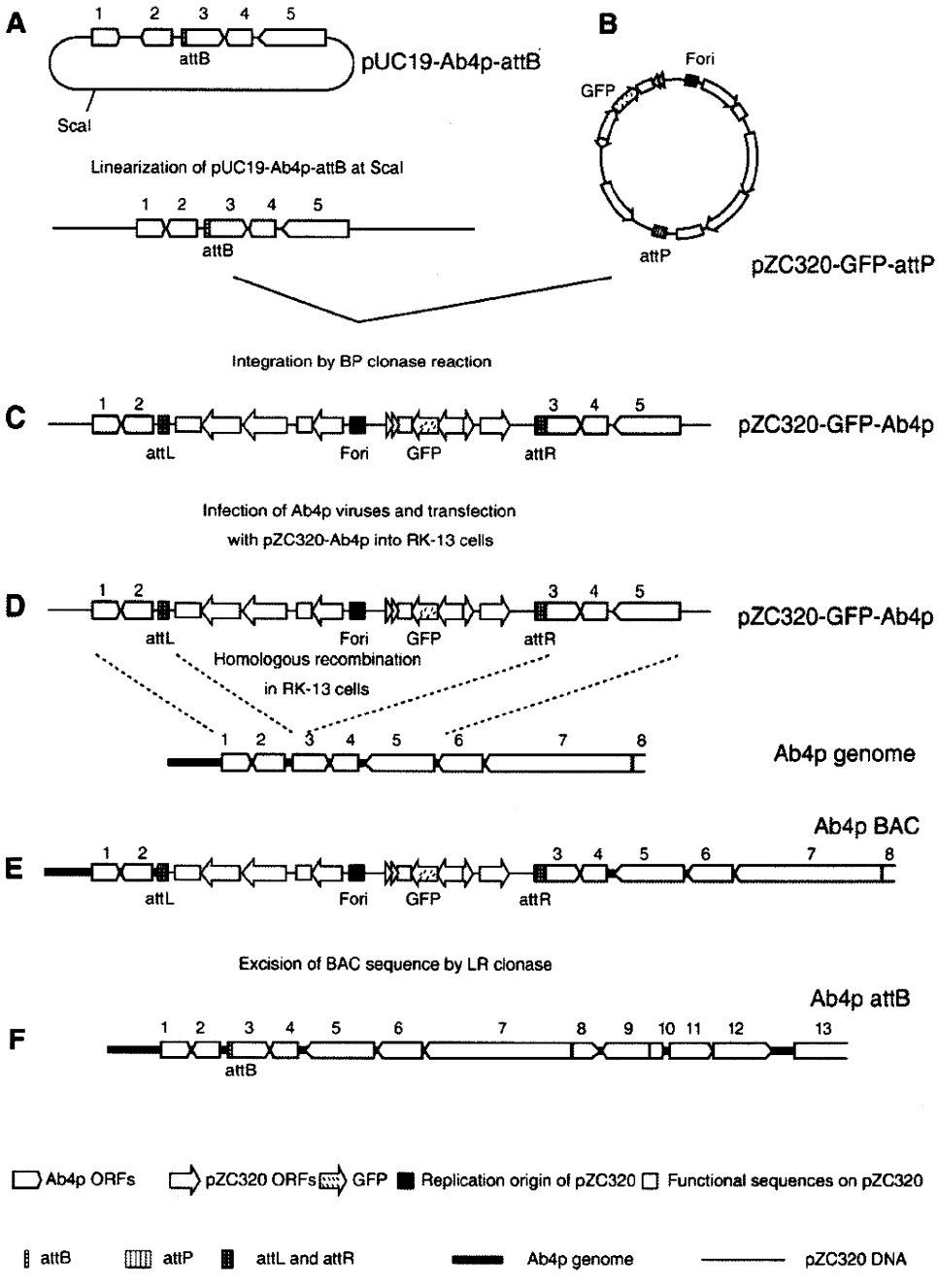

Fig. 1. Schematic diagrams of construction of Ab4p BAC and Ab4p attB. A pZC320-GFP-Ab4p (C) was constructed by BP clonase reaction between *attB* site in the pUC19-Ab4p-*attB* (A) and *attP* site in the pZC320-GFP-*attP* (B). Ab4p BAC virus (E) was constructed by homologous recombination in RK-13 cells (D). RK-13 cells were infected Ab4p and transfected with pZC320-GFP-Ab4p. Then, plaques containing the BAC virus were examined in MDBK cells by using GFP fluorescence as a marker. The desired virus plaque was identified and marked under fluorescent microscopy in order to pick up the plaque clone for further serial plaque purification. Ab4p BAC maintained in *E. coli* DH10β, which was generated by electroporation of circular viral DNA of Ab4p BAC. Ab4p attB DNA, which excised BAC sequence from Ab4p BAC DNA, was generated by LR clonase reaction (F). RK-13 cells were transfected with Ab4p attB DNA. Then, the purity of the plaques was examined in MDBK cells. The desired virus, which did not show fluorescence, was identified and marked under fluorescent microscopy for further cloning procedure.

mouse model. The inserted pZC320-GFP sequence of Ab4p BAC should be excised prior to pathogenicity evaluation of each virus gene of EHV-1 in the mouse model.

Deletion and characterization of ORF37 in EHV-1

The roles and significance of ORF37 of EHV-1 were investigated by using molecular recombination of Ab4p BAC. To construct an ORF37 deletion mutant, the ORF37 of pAb4p BAC was replaced with a prokaryotic selection marker, the rpsL-neo gene conferring streptomycin sensitivity and kanamycin resistance, by Red mutagenesis in *E. coli*. The resulting ORF37 negative Ab4p BAC mutant was termed pAb4pΔORF37 BAC (Figs. 4A and B).

The correct insertion of the rpsL-neo gene and deletion of ORF37 was confirmed by PCR and nucleotide sequencing. pAb4pΔORF37 BAC DNA, isolated from *E. coli*, was treated with LR clonase enzyme to excise the pZC320-GFP fragment and transfected into RK-13 cells to reconstitute the virus with ORF37-deletion, designated Ab4pΔORF37. To restore

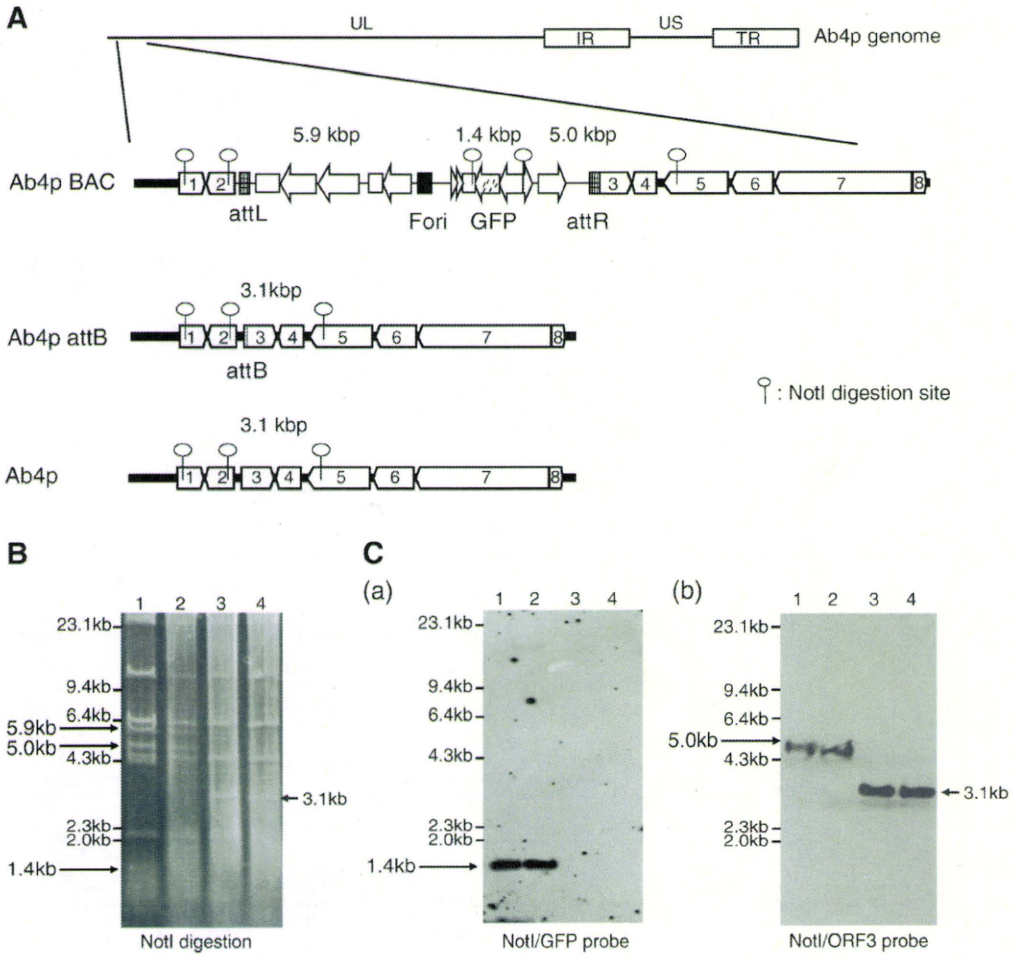

Fig. 2. Confirmation of Ab4p BAC and Ab4p *att*B by restriction digestion and Southern blotting. A: Location of the NotI digestion site in Ab4p BAC, Ab4p attB and Ab4p. B: NotI digestion of Ab4p BAC genome DNA in *E. coli* and virus (lanes 1 and 2), Ab4p attB (lane 3) and Ab4p genomes (lane 4). Ab4p BAC had fragments of about 5.9, 1.4 and 5.0 kbp containing BAC vector sequence. Ab4p attB and Ab4p had an approximately 3.1 kbp fragment but not the 5.9, 1.4 and 5.0 kbp fragments. C: Genomic DNAs from Ab4p BAC, Ab4p attB and Ab4p were digested with NotI and hybridized with probes specific for GFP (NotI/GFP probe, lanes 1 and 2) (a) or ORF3 (NotI/ORF3 probe, lanes 1, 2, 3 and 4) (b).

ORF37, homologous recombination of amplified PCR product of ORF37 and pAb4pΔORF37 BAC in DH10β resulted in replacement of rpsL-neo gene with ORF37-encoding sequence and reconstitution of a revertant BAC, pAb4pΔORF37R BAC. The ORF37 rescuant pAb4pΔORF37R BAC DNA, isolated from *E. coli*, was reacted with LR clonase to excise the BAC fragment and transfected into RK13 cells to reconstitute the ORF37 rescuant virus, Ab4pΔORF37R.

The genotypes of all generated and tested viruses were confirmed by restriction enzyme analyses using HincII and PvuII, nucleotide sequencing (data not shown), and PCR. When the ORF37 was present, it resulted in a PCR product of 955 bp. The 955 bp product was detected in cells infected with Ab4p, Ab4p attB and Ab4pΔORF37R viruses (Fig. 4C, lanes 1, 2 and 4). Insertion of the rpsL gene instead of ORF37 resulted in a product of 1420 bp in size in cells infected with ORF37 deletion mutant Ab4pΔORF37 (Fig. 4C, lane 3).

In vitro growth properties of ORF 37-negative mutants in cultured cell line

The *in vitro* growth properties of the generated ORF37-negative virus were analyzed in MDBK cells. To assess a possible contribution of ORF37 to the plaque formation of EHV-1, plaque areas of Ab4pΔORF37 were quantified and compared to those of parental Ab4p, AB4p attB and Ab4pΔORF37R. In three independent experiments, no significant difference was found in virus plaque sizes among wild-type, Ab4p attB, Ab4pΔORF37, and Ab4pΔORF37R (data not shown). The results indicate that the deletion of ORF37 in EHV-1 has no influence on plaque size. The virus titers in MDBK cells inoculated with all tested viruses were similar (Fig. 5). No differences were observed in the end-point virus titers between Ab4pΔORF37 and parental Ab4p, Ab4p attB and Ab4pΔORF37R.

Evaluation of growth activity by real-time RT-PCR

The growth activity of these viruses in MDBK cells was analyzed. The MDBK cells were infected with Ab4p, Ab4p attB, Ab4pΔORF37 and Ab4pΔORF37R. The growth activities of all viruses were evaluated through estimating ORF30 (DNA polymerase) RNA expression by real-time RT-PCR with using β-actin gene expression as a control. β-actin gene expression levels were the same among the MDBK cells infected by all viruses. The expression of ORF30 of Ab4pΔORF37 was nearly the same as that of other viruses (data not shown). From these data, we concluded that the ORF37 is completely dispensable for growth of EHV-1 in cultured cells.

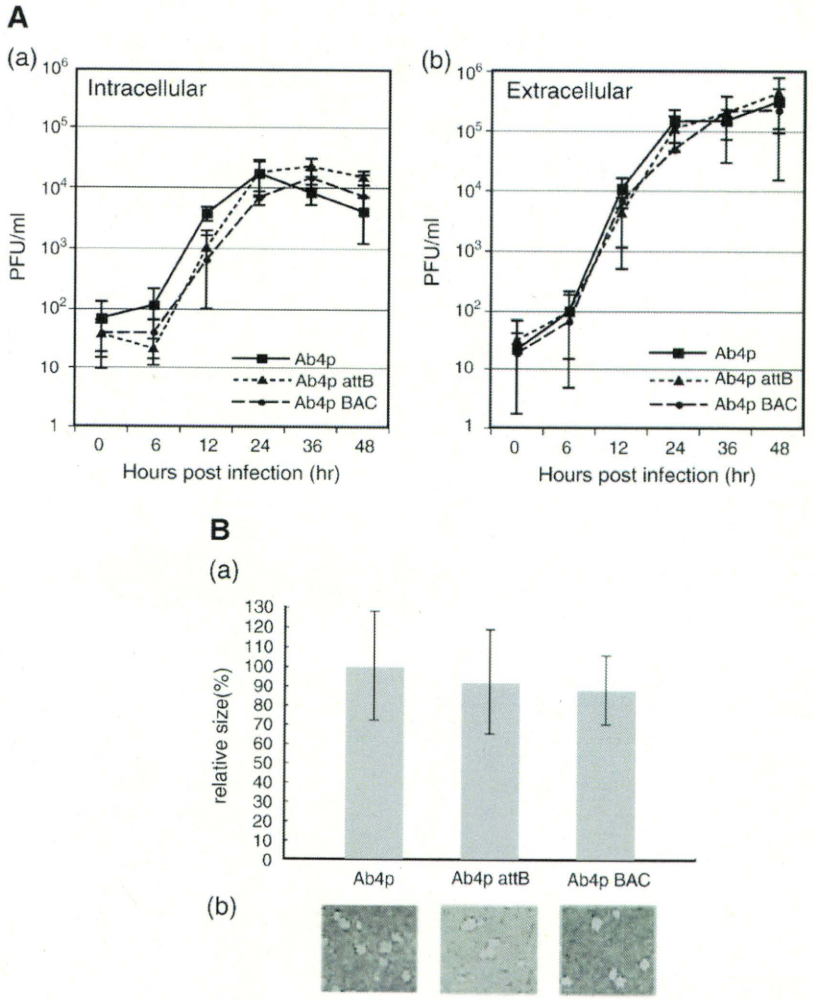

Fig. 3. Comparison of the *in vitro* growth properties of Ab4p, Ab4p BAC and Ab4p attB viruses. A: MDBK cells were infected with Ab4p, Ab4p BAC and Ab4p attB at an MOI of 0.1. At the indicated times after infection, cells and supernatant were harvested separately as described in Materials and methods. Intracellular (a) and extracellular (b) viruses were titrated by plaque formation on MDBK cells. The experiments were performed in triplicate. B: Relative plaque sizes of 50 randomly selected plaques of the Ab4p, Ab4p BAC and Ab4p attB. The plaques formed by Ab4p, Ab4p BAC and Ab4p attB had identical plaque sizes ($p<0.01$) (A) and the same morphology (B). Error bars are standard errors.

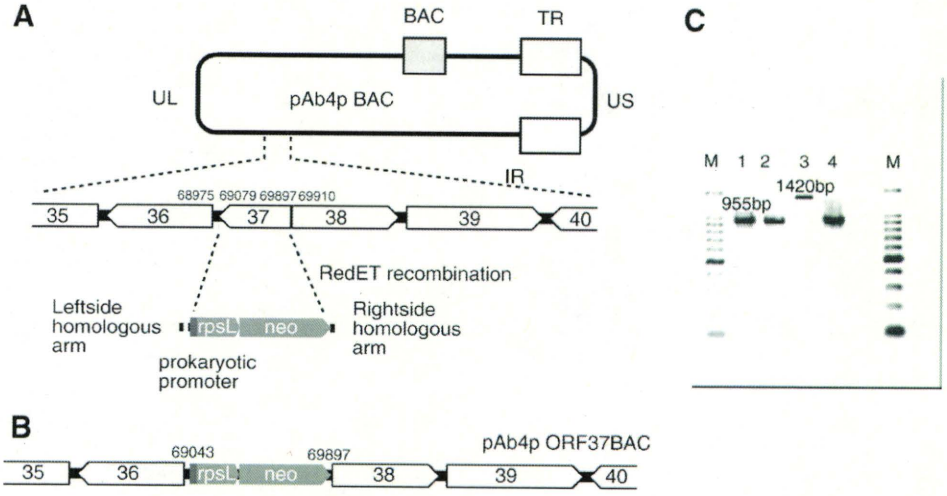

Fig. 4. PCR analysis of the generated recombinant viruses using primers ORF37-1 and ORF37-2. Intact ORF37 yields a fragment of 955 bp, whereas virus DNA containing the rpsL gene results in a fragment of 1420 bp. The molecular size marker is the 100-bp ladder (TOYOBO, Japan). PCR products from the different viruses were electrophoresed in 1% agarose gel. Markers (lane M) were included to assess the sizes of the PCR products. Lane 1: Ab4p, lane 2: Ab4p attB, lane 3: Ab4pΔORF37, lane 4: Ab4pΔORF37R, M: Molecular weight marker.

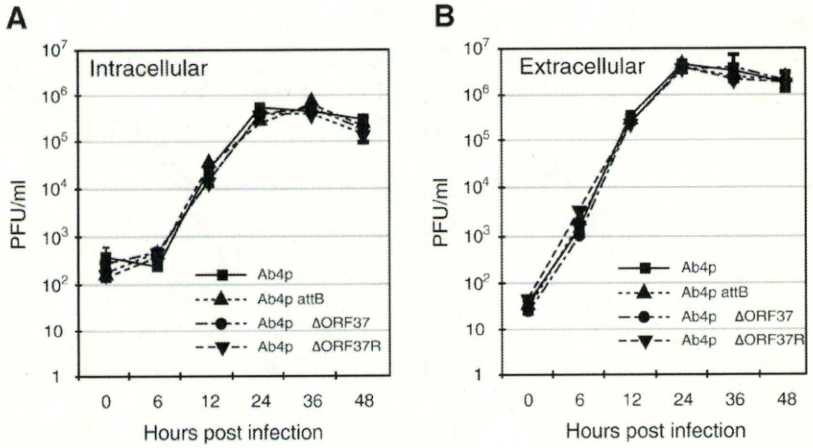

Fig. 5. Comparison of the *in vitro* growth curve of wild-type Ab4p and mutant viruses generated by BAC technology. MDBK Cells were infected at a MOI of 0.1. At the indicated times after infection, cells and supernatant were harvested separately as described in Materials and methods. Intracellular (A) and extracellular (B) viruses were titrated by plaque formation on MDBK cells. The experiments were performed in duplicate. Error bars are standard errors.

Effect of ORF37 deletion on transcription activities of ORFs 36, 38, 30 and 33

To evaluate the effects of the deletion of ORF37, transcript levels of two neighboring ORFs (ORF36 and 38) and distant two ORFs (ORF30 and 33) were measured in MDBK cells infected with Ab4p, Ab4p attB, Ab4pΔORF37 and Ab4pΔORF37R. β-actin levels in cells infected with the different strains were the same. ORF37 transcripts were not detected in cells infected with the deletion mutant, Ab4pΔORF37 (Fig. 6B). Deletion of ORF37 did not affect transcription levels of ORF36 (Fig. 6A), ORF30 and ORF33 (data not shown). Transcription level of ORF38 in Ab4pΔORF37 infected cells was one log order lower than that of other viruses until 4 h post infection and maintained the same from 6 h and later post infection (Fig. 6C).

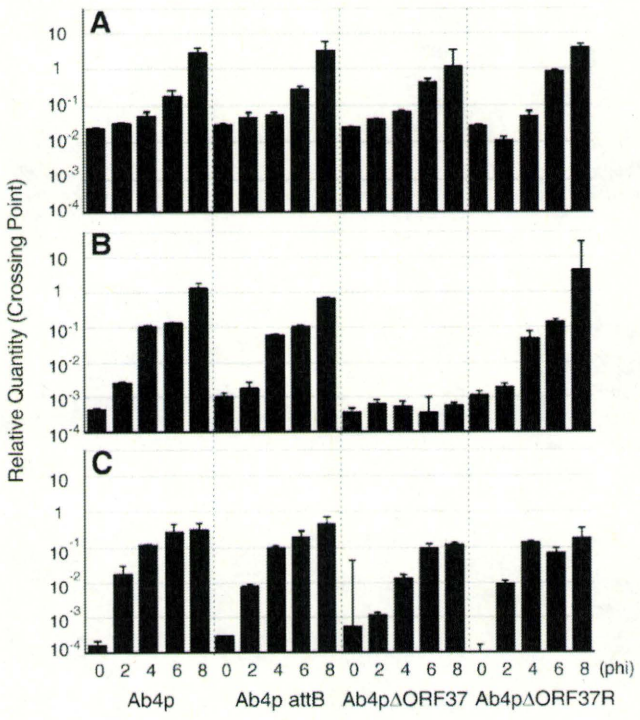

Fig. 6. Analysis of transcription activity of ORF36, ORF37 and ORF38 by real-time RT-PCR. Real-time RT-PCR analysis was performed by using RNAs from MDBK cells infected with Ab4p, Ab4p-attB, Ab4pΔORF37 and revertant virus at different times 0, 2, 4, 6 and 8 h post infection. The figure compares the transcription levels of theses viral genes in MDBK cells. Transcription activity of ORF36 (A), ORF37 (B) and ORF38 (C) were examined by real-time RT-PCR. Relative quantity was evaluated by crossing point method using with β-actin gene control.

Experimental infection of mice

To evaluate the role of ORF37 in the neuropathogenicity of EHV-1, CBA/N1 mice were inoculated with Ab4p, Ab4p attB, Ab4pΔORF37, and Ab4pΔORF37R. Mice that were inoculated with Ab4p, Ab4p attB and Ab4pΔORF37R showed nervous signs such as hyperactivity, arching the back and paralysis (Table 1). These symptoms started from 3-day post inoculation (dpi) in the Ab4p inoculated group and by 4 and 5 dpi in the Ab4p attB and Ab4pΔORF37R inoculated groups. Mice inoculated with Ab4pΔORF37 did not show any nervous signs and gained body weight throughout the observation period (Fig. 7). The body weights of mice inoculated with Ab4p, Ab4p attB and Ab4pΔORF37R decreased from 5, 8 and 8 dpi, respectively. From 7 to 13 dpi, mean body weights of mice inoculated with Ab4pΔORF37 were significantly larger than those of mice inoculated with Ab4p, Ab4p-attB or Ab4pΔORF37R.

Viruses were consistently recovered from the lungs from 2 to 7 dpi of mice inoculated with Ab4p, 2 to 6 dpi of mice inoculated with Ab4p attB and from 3 to 7 dpi of mice inoculated with Ab4pΔORF37R, respectively. On the other hand, the virus was recovered from 3 to 6 dpi in Ab4pΔORF37 inoculated mice. The viruses were recovered from the brain of mice inoculated with Ab4p, Ab4p attB from 3 to 6 dpi and Ab4pΔORF37 inoculated mice from 4 to 7 dpi, while the virus was recovered from Ab4pΔORF37 inoculated mice from 3 to 5 dpi with a

Table 1
The nervous symptoms of mice inoculated with Ab4p, Ab4p-attB, Ab4pΔORF37 and Ab4pΔORF37R.

Viruses	Days post inoculation													
	0	1	2	3	4	5	6	7	8	9	10	11	12	13
Ab4p#	−	−	−	+	+	+	+	+	+*	+*				
Ab4p attB	−	−	−	−	+	+	+	+	+	+	+	+*	+	+
Ab4p ΔORF37	−	−	−	−	−	−	−	−	−	−	−	−	−	−
Ab4p ΔORF37R	−	−	−	−	−	+	+	+	+	+	+	+	+	+*
Mock	−	−	−	−	−	−	−	−	−	−	−	−	−	−

#: Mice inoculated with Ab4p were sacrificed on 10-day post inoculation humanely.
−: No nervous signs such as hyperactivity, paralysis, arching of the back and lethargy.
+: Nervous signs such as hyperactivity, paralysis, arching of the back and lethargy.
*: A mouse died.

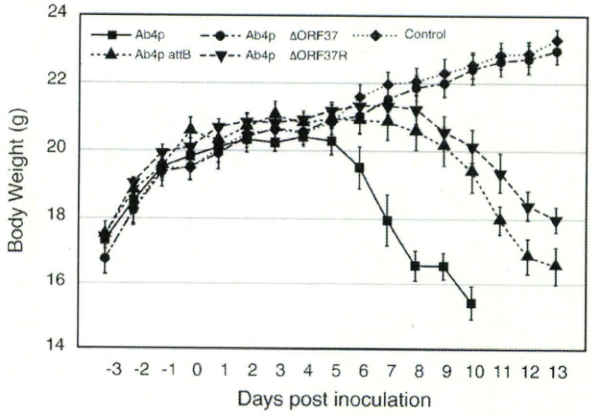

Fig. 7. Mean body weight curves of mice inoculated with Ab4p and mutant viruses. Mice in groups of four were infected intranasally with 1×10^5 pfu of the indicated virus. Mean body weights were measured from 3 days before inoculation (−3 dpi) to 13 dpi. Each data represents the mean of the body weight for the indicated group. Error bars indicate standard errors.

virus titer less than 1×10^2 pfu/g (Table 2). Virus DNA was detected in the lungs of mice inoculated with Ab4p from 2 to 10 dpi, Ab4p attB from 2 to 9 dpi, and Ab4pΔORF37R from 3 to 9 dpi. Virus DNA was detected in the brain of mice inoculated with Ab4p from 3 to 10 dpi, from 3 to 9 dpi in mice inoculated with Ab4p attB and from 4 to 8 dpi in mice inoculated with Ab4pΔORF37R, while virus DNA was detected from 3 to 8 dpi in the lungs and from 3 to 7 dpi in the brain of mice inoculated with Ab4pΔORF37 (Table 2).

None of the mice showed gross pathological changes at necropsy, while the histopathological findings of the lungs showed interstitial pneumonia in the lungs of all mice examined but not in mock inoculated mice (data not shown). The brains of mice infected with Ab4pΔORF37 did not show any histopathological changes or signs of encephalitis nor meningitis, while the brains of mice infected with wild-type Ab4p, Ab4p attB and Ab4pΔORF37R showed non-suppurative encephalitis and meningitis (Fig. 8). The histopathological lesions consisted of degeneration and necrosis of the neurons, lymphocytic cell infiltration, perivascular cuffing, meningitis and gliosis (Table 3).

In vitro growth properties of ORF 37-negative mutant in cultured mouse neurons

The intracellular and extracellular virus titers of Ab4pΔORF37 were one order of magnitude lower than those of parental Ab4p, Ab4p attB and Ab4pΔORF37R in mouse neuronal cells (Fig. 9), indicating that the deletion of ORF37 affected EHV-1 multiplication in neuronal cells.

Discussion

We established an EHV-1 BAC clone, pAb4p BAC, based on the neuropathogenic strain Ab4p. Our pAb4p BAC has no deletion of genes, because the BAC vector (pZC320-GFP sequence) was inserted into the intergenic region between ORF2 and ORF3 of Ab4p using the lambda insertion–excision system. Thus, pAb4p BAC should maintain the complete original genetic information of Ab4p.

The BAC vector (a 9.2 kb pZ320-GFP sequence) was inserted into the intergenic region between ORF2 and ORF3 in pAb4p BAC. The function of EHV-1 ORF2 is unknown. VZV ORF2, which is homologous to the EHV-1 ORF3 gene, might not have a role in virus replication or establishment of latency (Sato et al., 2002; Zhang et al., 2007). The EHV-1 ORF3 product was suggested to play a role in the assembly of the virus (Harty et al., 1993). Insertion of a large fragment, such as a BAC vector, in virus genome might affect the virological characteristics by inefficient packaging (Smith and Enquist, 1999; Wagner et al., 1999) or by interfering with the transcription of neighboring genes. The present transcription analyses on ORF2, ORF3 and other viral genes showed a decrease of transcripts in Ab4p BAC. The BAC vector insertion might affect the transcription of genes on both side genes of BAC insertion site and other genes. On the other hand, in Ab4p attB infected cells, a decrease in the transcription was observed only for ORF3. Ab4p attB behaved like the wild-type Ab4p in terms of *in vitro* growth and neuropathogenicity in mouse, suggesting that low transcriptions of ORF3 did not affect the viral growth in MDBK cells and is not associated with the neuropathogenicity of EHV-1 in mouse. Therefore Ab4p attB can be regarded as equivalent to the wild-type Ab4p.

In this study, we constructed Ab4p BAC using BP and LR clonase. This reaction is based on the lambda site-specific recombination system, which is a reaction between *att*L and *att*R or *att*B and *att*P. The clonase reactions are unidirectional, and are effective with both insertions and deletions unlike the Cre/loxP system whose ability to insert fragments is low (Thomson et al., 2003). We were able to construct Ab4p BAC more efficiently than we could by normal subcloning using restriction enzymes and ligase. Additionally, the BAC vector in Ab4p BAC was flanked by *att*L and *att*R. Therefore, the BAC vector was easy to excise by the LR clonase reaction and to insert by BP clonase.

CBA mouse showed brain lesions similar to those observed in EHV-1 infected horses exhibiting neurological signs (Frampton et al., 2004). Additionally, much is known about the genetic and the biological characteristics of the CBA mice. Therefore, CBA mice seem to be a good model for evaluating the neuropathogenicity of the Ab4p BAC system. The pathogenicity of Ab4p attB was similar to that of the wild-type Ab4p in mice. Especially, the same nervous symptoms were observed in each mice inoculated with Ab4p and Ab4p attB, respectively. These results suggest that Ab4p attB, which contains attB sequence, can be used to evaluate the neuropathogenesis of EHV-1.

Table 2
Virus titration and DNA detection in mice organs inoculated with Ab4p, Ab4p attB, Ab4p ΔORF37 and Ab4p ΔORF37R.

Viruses	Organs	Day post inoculation										
		0	1	2	3	4	5	6	7	8	9	10
Ab4p	Brain	−/−*	−/−	−/−	2×10^2/+	4×10^3/+	3×10^3/+	4×10^2/+	−/+	−/+	−/+	−/+
	Lung	−/−	−/−	5×10^2/+	3×10^2/+	2×10^4/+	2×10^4/+	1×10^3/+	2×10^3/+	−/+	−/+	−/+
Ab4p attB	Brain	−/−	−/−	−/−	1×10^2/+	5×10^3/+	2×10^2/+	1×10^2/+	−/+	−/+	−/+	−/−
	Lung	−/−	−/−	2×10^2/+	1×10^2/+	1×10^4/+	1×10^3/+	1×10^3/+	−/+	−/+	−/+	−/−
Ab4p ΔORF37	Brain	−/−	−/−	−/−	−/+	−/+	−/+	−/+	−/+	−/−	−/−	−/−
	Lung	−/−	−/−	−/−	−/+	3×10^2/+	2×10^3/+	3×10^3/+	−/+	−/+	−/−	−/−
Ab4p ΔORF37R	Brain	−/−	−/−	−/−	−/−	3×10^2/+	5×10^2/+	2×10^3/+	1×10^3/+	−/+	−/−	−/−
	Lung	−/−	−/−	−/−	3×10^2/+	2×10^2/+	1×10^4/+	3×10^2/+	4×10^2/+	−/+	−/+	−/−

*: Virus titer in pfu per gram of organ/virus DNA detection.
+: Virus DNA was detected.
−: Virus titer was less than 1×10^2 pfu per gram or virus DNA was not detected.

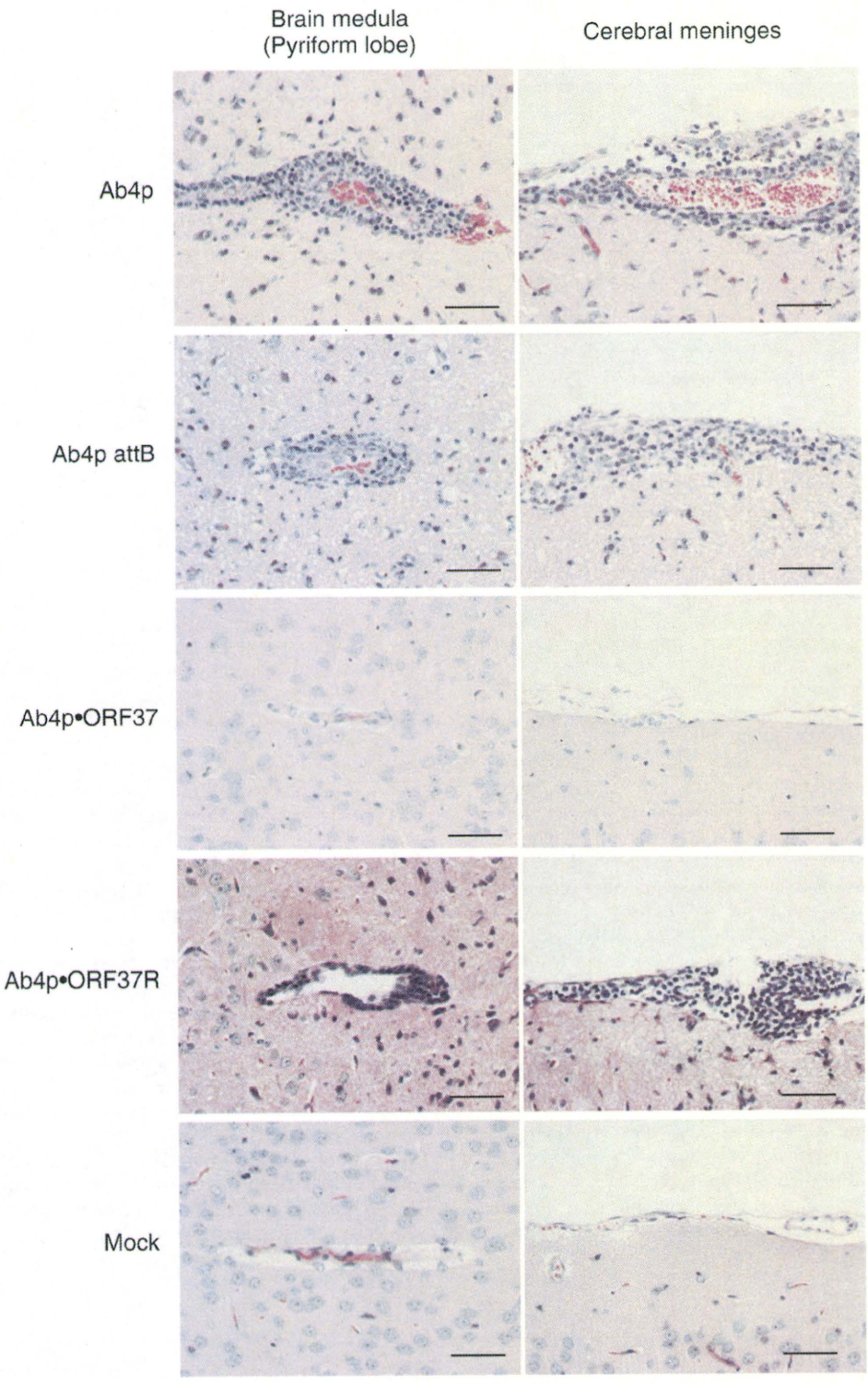

Fig. 8. Histological sections of brains of mice infected with wild-type, Ab4p attB, Ab4pΔORF37, Ab4pΔORF37R and mock. Mice were infected intranasally with the indicated doses. Mice brains were stained with hematoxylin and eosin. Slides were inspected by light microscopy and photographed. A bar indicates 10 μm.

A number of herpesvirus genes have been shown to be nonessential for growth in cultured cells. However, when viral mutants were tested in certain animal models, several of these genes proved to be important in promoting viral replication and disease in vivo (Subak-Sharpe and Dargan, 1998; Visalli and Brandt, 2002; Ward and Roizman, 1994). We described the isolation of an ORF37 replacement mutant that is viable *in vitro* yet shows significant attenuation in mice models.

Analysis of the role of the ORF37 gene in the viral life cycle *in vitro* and in vivo has been complicated by the fact that certain mutations in ORF37 can affect the expression of the ORF38 (thyamidine kinase) gene (Jacobson et al., 1989; Meignier et al., 1988; Sears et al., 1985).

Table 3
The pathological lesions of mice inoculated with Ab4p, Ab4p attB, Ab4p ΔORF37 and Ab4p ΔORF37R.

Viruses	Neuronal degeneration	Meningitis	Perivascular cuffing	Glial reaction	Interstitial pneumonia
Ab4p	+++	+++	+++	+	+++
Ab4p attB	+++	+++	++	+	++
Ab4p ΔORF37	+	−	−	−	+
Ab4p ΔORF37R	+++	++	++	−	++

−: No lesion; +: mild lesions; ++: moderate lesions; +++: severe lesions.

However, the rpsL-neo gene replacement, which was used to delete the ORF37, had no obvious effect on expression or function of ORF38 or ORF36, or on the transcription activities of ORF30 (DNA polymerase) and ORF33 (envelope glycoprotein B). Therefore phenomena observed in this work could be regarded to be caused by the deletion of ORF37 itself.

Our results showed that the ORF37 protein is required for EHV-1 to express neuropathogenicity in mouse, although the ORF37 product is dispensable for viral replication in cell cultures. Also the results showed that the virus mutant, Ab4pΔORF37, showed normal multiplication curves and the same plaque morphology in cell cultures as the parental EHV-1 virus and other recombinant viruses used. On the other hand, the ability of the EHV-1 ORF37 deletion mutant to replicate in cultivated mouse neural cells derived from cerebral cortex was significantly impaired. The virus titers of Ab4pΔORF37 were one order magnitude lower than those of parental Ab4p, Ab4p attB and Ab4pΔORF37R. These results suggested that the ORF37 product (UL24) plays a role in the multiplication of EHV-1 in neural cells by unknown mechanism, although it is not needed in the ordinary cell cultures such as MDBK, FEK and RK13 cells. Further studies are needed to understand why ORF37 is needed for replication in mouse neural cells but not in ordinary cells cultures.

The role of the ORF37 gene in vivo was assessed by intranasal inoculation of parental and recombinant viruses into CBA/N1mice. Our results showed the absence of neurological signs and the normal body weight gain, with no mortalities in the mice inoculated with the Ab4pΔORF37 mutant. The histopathological findings showed no lesions in the brain and mild lesions in the lungs of the mice inoculated with Ab4pΔORF37 mutant. Moreover, Ab4pΔORF37 replication in the brain and lungs was impaired as shown in Table 2, indicating that ORF37 protein is required for efficient expression of EHV-1 pathogenesis in the brain and lungs.

In summary, BAC cloning technology has opened new avenues for the manipulation of several herpesvirus genomes. The feasibility of mutagenesis of the EHV-1 BAC clone has been studied in this paper. Our findings reported here revealed no significant difference between wild-type EHV-1 and ORF37 negative mutant in their replication cycle in cell culture. However, there is one order of magnitude decrease in the mouse neuron cells inoculated with Ab4pΔORF37 than those inoculated with Ab4p, Ab4p attB and Ab4pΔORF37R viruses. The deletion of ORF37 did not affect on the transcription activities of the neighboring genes and other genes. The mice inoculated with an Ab4pΔORF37 mutant did not show neurological symptoms, death and body weight loss. Taken together, the findings at the present study indicate that ORF37 of EHV-1 is one of the neuropathogenicity factors of EHV-1.

Materials and methods

Virus and cells

EHV-1 Ab4p strain (Gibson et al., 1992), which was kindly provided by Dr. A. J. Davison, Glasgow University, Scotland, was used. The virus was propagated in fetal equine kidney (FEK) cells. Other cells used in this study were Madin–Darby bovine kidney (MDBK) and Rabbit kidney 13 (RK-13) cells. All of these cells were cultivated with Eagle's minimum essential medium (MEM) (Nissui, Tokyo, Japan) supplemented with 5–10% fetal bovine serum (FBS) and 100 U/ml penicillin and 100 μg/ml streptomycin.

E. coli and plasmids

DH10β strain of *E. coli* was used for construction and maintenance of BAC clones. The pZC320 plasmid (Shi and Biek, 1995) was used as the basis of BAC vector, which was kindly provided by National Institute of Genetics (Mishima, Japan). Other plasmids used were pUC19 (TAKARA, Shiga, Japan) and pEGFP-N1 (Clontech, U.S.A.).

Construction of BAC plasmids

A fragment of the Ab4p genome corresponding nucleotide (nt) 812 to 4722 was amplified by PCR using the following primers: fORF1–5 5′-ACA GCG AAT TCA CAT TAG TTG CCA CGC TTC T-3′ and rORF1–5 5′-CAC TCG GAA TTC CCA CCT TCA TGT TCG TGA TG-3′ and was cloned at pUC19 EcoRI site (pUC19-Ab4p). The Ab4p fragment contains a single ClaI site (at nt 2838), which is located in the intergenic region between ORF2 and ORF3. A ClaI-*att*L-*att*R-ClaI polynucleotide (324 bp) was synthesized in Dragon Genomics Center (Mie, Japan). This polynucleotide fragment was inserted at pUC19-Ab4p ClaI site (pUC19-Ab4p-*att*LR). A pUC19-Ab4p-*att*B was constructed from pUC19-Ab4p-*att*LR by removing the stuffed fragment with LR clonase

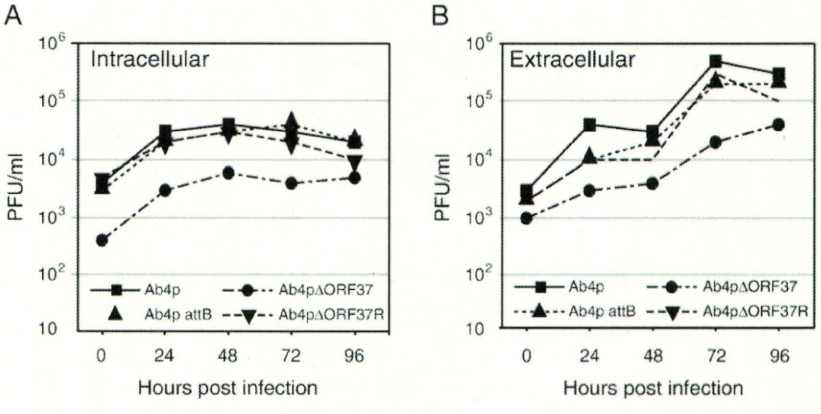

Fig. 9. Growth curve of wild-type Ab4p and EHV-1 mutant viruses by using mouse neurons, CX (M) Cells. The neuron cells were infected at a MOI of 1. At the indicated times after infection, cells and supernatant were harvested separately as described in Materials and methods. Intracellular (A) and extracellular (B) viruses were titrated by plaque formation on MDBK cells. The experiments were performed in duplicate. Error bars are standard errors.

reaction (Fig. 1A). LR clonase reaction was performed according to the manufacturer's instructions of Gateway LR Clonase Enzyme Mix (Invitrogen, Tokyo, Japan). The GFP expression cassette consisted of human cytomegalovirus immediate early promoter, GFP gene and an SV40 early mRNA polyadenylation signal in pEGFP-N1 was cloned in BamHI–SphI sites of pZC320 multi cloning site (pZC320-GFP). Additionally, an *att*P sequence was amplified from lambda phage DNA (TAKARA BIO, Shiga, Japan) by PCR using the following primers: f*att*P 5′-AGC GAA TTC AAT GCT CTG TTA CAG GTC A-3′ and r*att*P 5′-TAC GCG TCT CGA CGA AAT CAA ATA ATG ATT TTA TTT TGA CTG-3′. The *att*P sequence fragment was cloned in EcoRI–SalI sites of pZC320-GFP (pZC320-GFP-*att*P) (Fig. 1B). The pUC19-Ab4p-*att*B was linearized by digestion with ScaI. The pZC320-GFP-*att*P was inserted into linearized pUC19-Ab4p-*att*B by BP clonase reaction (pZC320-Ab4p) (Fig. 1C). BP clonase reaction was performed according to the manufacturer's instructions of Gateway BP Clonase Enzyme Mix (Invitrogen, Tokyo, Japan).

Isolation of Ab4p BAC virus

RK-13 cells in a 24-well plate was infected by Ab4p at a multiplicity of infection (MOI) of 0.1. After 60 min of adsorption, 1.0 μg of the linear pZC320-GFP-Ab4p DNA per well was transfected into the RK-13 cells by lipofectamine 2000 (Invitrogen, Tokyo, Japan) and incubated at 37 °C (Fig. 1D). After 5–7 days cultivation, supernatant was collected. The supernatant was inoculated to MDBK cells. After 60 min of adsorption, the MDBK cells were covered by MEM containing 1.5% of carboxymethylcellulose and incubated for 4–5 days at 37 °C. Using GFP fluorescence as a marker, the desired virus (Ab4p BAC) identified and selected under fluorescent microscopy (Fig. 1E). The Ab4p BAC virus was purified by three rounds of plaque purification.

Transformation of E. coli and mutagenesis of pAb4p

Competent *E. coli* DH10β (Invitrogen, Tokyo, Japan) was used for transformation. Circular viral DNA of Ab4p BAC was isolated from infected FEK cells by the Hirt method (Hirt, 1967). Circular Ab4p BAC DNA was electroporated into DH10β by using a Bio-Rad GenePulser (Bio-Rad, Tokyo, Japan) with 0.1 cm cuvettes, 1.3 kV, 10 μF and 100 Ω. The Ab4p BAC containing clones were selected by growth on LB agar plates containing ampicillin at 50 μg/ml. Resistant bacterial clones were isolated and grown overnight in LB medium containing ampicillin. The presence of Ab4p BAC as a plasmid (pAb4p BAC) was confirmed by extraction of large plasmid DNA with Nucleo Bond BAC 100 kit (MACHEREY-NAGEL, USA) and restriction enzyme digestion (NotI).

For modification of pAb4p BAC, Red mutagenesis was used (Datsenko and Wanner, 2000; Thomson et al., 2003). Briefly, competent *E. coli* DH10β harboring pAb4p BAC and the Red/ET plasmid pKD46 [DH10β (pAb4p, pKD46)] were grown in Luria–Bertani broth (LB) with tetracycline (30 μg/ml), ampicillin (50 μg/ml), and L-arabinose (0.1% final concentration) at 30 °C to an optical density at 600 nm of 0.6 and then made electrocompetent exactly as previously described (Datsenko and Wanner, 2000). To delete ORF37 in pAb4p BAC, ORF37 was replaced with the rpsL-neo cassette (rpsL-neo gene) conferring streptomycin sensitivity and kanamycin resistance, resulting in recombinant BAC termed pAb4pΔORF37 BAC (Fig. 4) as follows. A pair of primer-1 (5′-GGT CTT TAG CTT CGA TCT TAG TGT TTA TAC TTG CGT GTA GGC GCG CCG AC**G GCC TGG TGA TGA TGG CGG GAT CG**-3′) and primer-2 (5′-CTC CGT CGA GCT TCC CCG GAA GGT ACG CGA GCC GCC ATT GAT TTC TGA AA**T CAG AAG AAC TCG TCA AGA AGG CG**-3′) containing 50-nucleotide homology arms bordering the desired deletion from position 69043 to 69897 of gene 37 and 24 nucleotides (in boldface) for amplification of the rpsL-neo cassette sequences was designed to be used for amplification of the insertion fragment with the use of the rpsL-neo template DNA (Gene Bridges) as a template DNA. The resulting 1420 bp PCR fragment was purified from agarose gel (QIAquick gel extraction kit; QIAGEN) and electroporated into DH10β (pAb4p, pKD46) using 0.1-cm cuvettes (Bio-Rad Laboratories) under standard electroporation conditions (1.35 kV/cm, 600 Ω 10 μF). After electroporation, cells were grown in 1 ml of LB for 70 min at 37 °C and plated onto LB agar plates containing 50 μg/ml of ampicillin, 30 μg/ml tetracycline and 15 μg/ml of kanamycin. Resistant colonies were picked into liquid LB medium, grown at 37 °C, and small-scale preparations of mutant pAb4p-DNA (pAb4pΔORF37 BAC) were obtained by alkaline lyses of *E. coli* (Sambrook et al., 1989) to be confirmed by PCR and to be digested with various restriction enzymes.

Revertant virus construction

To replace the rpsL-neo gene with the ORF37 gene in the pAb4pΔORF37 BAC, DH10β (pAb4pΔORF37, pKD46) were grown in Luria–Bertani broth (LB) with tetracycline (30 μg/ml), ampicillin (50 μg/ml), kanamycin (15 μg/ml) and L-arabinose (0.1% final concentration) at 30 °C to an optical density at 600 nm of 0.6 and then made electrocompetent as previously described (Datsenko and Wanner, 2000). ORF37 was amplified by PCR with a pair of primer-3 (5′-GGT CTT TAG CTT CGA TCT TAG TGT TTA TAC TTG CGT GTA GGC GCG CCG AC-3′) and primer-4 (5′-CTC CGT CGA GCT TCC CCG GAA GGT ACG CGA GCC GCC ATT GAT TTC TGA AA-3′) including 50-nucleotide homology arms bordering the desired deletion from position 69043 to 69897 of ORF37. The resulting 955 bp PCR fragment was purified by agarose gel electrophoresis (QIAquick gel extraction kit; QIAGEN) and electroporated into DH10β (pAb4pΔORF37, pKD46) using 0.1 cm cuvettes (Bio-Rad Laboratories) under standard electroporation conditions (1.35 kV/cm, 600 Ω, 10 μF). After electroporation, cells were grown in 1 ml of LB for 70 min at 37 °C and plated onto LB agar plates containing 50 μg of ampicillin/ml, 50 μg of streptomycin. Double resistant colonies were picked into liquid LB medium, grown at 37 °C. Small-scale preparations of mutant DNA of pAb4pΔORF37R BAC were obtained by alkaline lyses of *E. coli* (Sambrook et al., 1989), confirmed by PCR, digested with various restriction enzymes.

Regeneration of infectious Ab4p BAC, Ab4p attB, Ab4pΔORF37 and Ab4pΔORF37R viruses

DNA was extracted by using a Nucleo Bond BAC 100 kit (MACHEREY-NAGEL, USA) from each BAC culture. For Ab4p BAC, 1 μg of pAb4p BAC DNA was transfected into RK-13 cells in a 24-well plate by lipofectamine 2000 (Invitrogen) and incubated at 37 °C. Then, Ab4p BAC was isolated as described above. For Ab4p attB, Ab4pΔORF37 and Ab4pΔORF37R, the DNAs were constructed by LR clonase reaction, which excises the BAC fragment from each BAC DNA. Then Ab4p attB, Ab4pΔORF37 and Ab4pΔORF37R viruses were generated with the methods used for regeneration of Ab4p BAC virus.

Virus growth kinetics and plaque area determinations

Titers of the viruses were determined by infecting MDBK cells at a multiplicity of infection (MOI) of 0.1 for virus growth kinetics as described by Pearson and Coen (2002). Confluent monolayers of MDBK cells in 24-well plates were infected with the Ab4p, Ab4p attB, Ab4pΔORF37 and Ab4pΔORF37R. Supernatant and cells were then collected at 0, 6, 12, 24, 36 and 48 h post infection each. A cell pellet was resuspended in the same volume of MEM to be frozen–thawed twice to release cell-associated virus. The titer of each sample was assessed by plaque assay by of MDBK cells. Plaque areas were measured after plating of the viruses on MDBK cells and 3 days of incubation at 37 °C under a 0.6% methylcellulose overlay. For each virus, plaque areas of at least 50 plaques for each experiment were determined in triplicate using the ImageJ 1.28 software that is freely available from the National Institutes of Mental Health webpage

(http://rsb.info.nih.gov/ij/docs/intro.html). Virus titers and plaque areas were statistically analyzed by an analysis of variance (ANOVA).

Virus growth kinetics in mouse neurons

To compare viral growth in the neurons, CX (M) cells (Sumitomo Bakelite, Tokyo, Japan) derived from mouse cerebral cortexes were cultured in 24-well plates coated with poly-L-lysine (Sumitomo Bakelite) in neuron culture medium (Sumitomo Bakelite, Tokyo, Japan). Titers of the various viruses were determined by infecting CX (M) cells at 1 MOI. The supernatant and cells were separately harvested at the indicated timing and virus titers were determined by plaque assay on MDBK cells after freeze and thaw cycles as described previously (Yamada et al., 2008).

Analysis of transcription kinetics by real-time RT-PCR

For analysis of transcription activity of ORF37, MDBK cells were infected with Ab4p, Ab4p-attB, Ab4pΔORF37 and Ab4pΔORF37R, resulting in 1 MOI. Total RNA was extracted by using Nucleospin RNA kit (MACHEREY-NAGEL, USA) from the infected and uninfected MDBK cells harvested at 0, 2, 4, 6 and 8 h post infection. Then 1.5 μg of RNA was heated at 95 °C for 5 min for denaturation, combined with reverse transcriptase master mix consisting of 4 μl of 5 × RT buffer (TOYOBO, Osaka, Japan), 5 mM of dNTP (TAKARA), 25 pmol of random primer (TOYOBO), 40 U of RNase inhibitor (TOYOBO) and 50 U of reverse transcriptase (TOYOBO). The reaction mixture was incubated at 30 °C for 10 min, 42 °C for 40 min followed by incubation at 99 °C for 5 min to stop the reaction. A real-time PCR assay was carried out using 12.5 μl of SYBR Premix Ex Taq (TAKARA), 10 μM of specific primers and 10 ng of cDNA in the Thermal Cycler Dice Real Time System (TAKARA). Primers sequences are for ORF37 (ORF37A 5′-CCG CAG CTG GAA ATA AAC TC-3′ and ORF37B 5′-CCT GCA CCA TAT CAC GTT TG-3′), ORF36 (ORF36A 5′-CAC CTC CCT GTT GGC TAT GT-3′ and ORF36B 5′-TTC TCA CGG AAG ACC AAA CC-3′), ORF38 (ORF38A 5′-ACT GGC GGA CTC TCT TTG AA -3′ and ORF38B 5′-GTC TCC GAT GAG GTA GCG AG-3′), ORF33 (ORF33A 5′-TTG TTA GAG CCG TAC CCA CC-3′ and ORF33B 5′-AAA GTC TCC ATC CTC AGC GA-3′) and ORF30 (DNA polymerase) primers (ORF30A 5′-GTC AGG CCC ACA AAC TTG AT-3′ and ORF30B 5′-ACT CGG TTT ACG GAT TCA CG-3′). Relative quantities were measured by the ΔΔCt method (Livak and Schmittgen, 2001).

Evaluation of growth activity by real-time PCR

The growth activities of the viruses and β-actin gene in MDBK cells which were infected with Ab4p, Ab4p attB, Ab4pΔORF37 and Ab4pΔORF37R, were evaluated by real-time PCR. Total DNA was extracted from the infected and uninfected MDBK cells harvested at 0, 2, 4, 6 and 8 h post infection. The growth activities of all viruses were evaluated through estimating a copy number of ORF30 (DNA polymerase) DNA with β-actin gene control by real-time PCR as described above.

Animal experiments

Animal experiments were conducted as described previously (Ho and Mocarski, 1988; Osterrieder et al., 1996; Fukushi et al., 2000). Briefly, four-week-old specific pathogen free (SPF) male CBA/N1 mice (26 mice per each virus and control) were inoculated with a virus preparation by the intranasal route at 1×10^5 pfu per head. Behavior and body weight of each mouse were observed from 3 days before the inoculation to the end of the period. Body weights were evaluated by analysis of variance and multiple comparisons of the groups. Two mice from each group were euthanized every day from 1 to 10 dpi for virus isolation and DNA detection. Lungs and the brain were used for virological assay. All experiments were conducted under the guidelines for animal experiments in Gifu University with certification by the committee of the Faculty of Applied Biological Sciences, Gifu University.

Tissues were homogenized in MEM at 10% (w/v). The homogenates were centrifuged at 3000 rpm for 10 min to remove the cellular debris. Supernatant was serially 10-fold diluted in MEM. A volume of 0.1 ml per well was inoculated onto a confluent MDBK monolayer in 24-well plates. Virus titers were determined by plaque assay. The detection limit in the organ homogenates was 1×10^2 pfu per gram of a mouse organ. DNA was extracted with a Sepagene kit for virus DNA detection in mice organs (Sanko Junyaku, Japan). Viral DNA was detected by using primers for ORF37 and primers for rpsL-neo gene for the mutant virus. For histopathology, brains and lungs were collected in buffered formalin and processed for histopathological analysis (Fukushi et al., 2000; Leist et al., 1989).

Acknowledgments

This study was supported by the Japan Society for the Promotion of Science, Grant-in-Aid for Scientific Research (B) for 17380181 and 21380179. The first author is grateful to the Egyptian Ministry of Higher Education, which supports him to study PhD abroad.

References

Allen, G.P., Bryans, J.T., 1986. Molecular epizootiology, pathogenesis, and prophylaxis of equine herpesvirus-1 infections. Prog. Vet. Microbiol. Immunol. 2, 78–144.
Allen, G.P., Yeargan, M.R., Turtinen, L.W., Bryans, J.T., McCollum, W.H., 1983. Molecular epizootiologic studies of equine herpesvirus-1 infections by restriction endonuclease fingerprinting of viral DNA. Am. J. Vet. Res. 44, 263–271.
Awan, A.R., Chong, Y.-C., Field, H.J., 1990. The pathogenesis of equine herpesvirus type 1 in the mouse: a new model for studying host responses to the infection. J. Gen. Virol. 71, 1131–1140.
Blakeney, S., Kowalski, J., Tummolo, D., DeStefano, J., Cooper, D., Guo, M., Gangolli, S., Long, D., Zamb, T., Natuk, R.J., Robert, J.V., 2005. Herpes simplex virus type 2 UL24 gene is a virulence determinant in murine and guinea pig disease models. J. Virol. 79, 10498–10506.
Borchers, K., Thein, R., Sterner-Kock, A., 2006. Pathogenesis of equine herpesvirus-associated neurological disease: a revised explanation. Equine Vet. J. 38, 283–287.
Brune, W., Messerle, M., Koszinowski, U.H., 2000. Forward with BACs: new tools for herpesvirus genomics. Trends Genet. 16, 254–259.
Chang, W.L., Barry, P.A., 2003. Cloning of the full-length rhesus cytomegalovirus genome as an infectious and self-excisable bacterial artificial chromosome for analysis of viral pathogenesis. J. Virol. 77, 5073–5083.
Csellner, H., Walker, C., Love, D.N., Whalley, J.M., 1998. An equine herpesvirus 1 mutant with a lacZ insertion between open reading frames 62 and 63 is replication competent and causes disease in the murine respiratory model. Arch. Virol. 143, 2215–2231.
Datsenko, K.A., Wanner, B.L., 2000. One-step inactivation of chromosomal genes in *Escherichia coli* K-12 using PCR products. Proc. Natl. Acad. Sci. U. S. A. 97, 6640–6645.
Frampton Jr., A.R., Smith, P.M., Zhang, Y., Grafton, W.D., Matsumura, T., Osterrieder, N., O'Callaghan, D.J., 2004. Meningoencephalitis in mice infected with an equine herpesvirus 1 strain KyA recombinant expressing glycoprotein I and glycoprotein E. Virus Genes 29, 9–17.
Fukushi, H., Taniguchi, A., Yasuda, K., Yanai, T., Masegi, T., Yamaguchi, T., Hirai, K., 2000. A hamster model of equine herpesvirus 9 induced encephalitis. J. Neurovirol. 6, 314–319.
Gibson, J.S., Slater, J.D., Field, H.J., 1992. The pathogenicity of Ab4p, the sequenced strain of equine herpesvirus-1, in specific pathogen-free foals. Virology 189, 317–319.
Goodman, B.L., Loregian, A., Perkins, A.G., Nugent, J., Buckles, L.E., Mercorelli, B., Kydd, H.J., Palu, G., Smith, C.K., Osterrieder, N., Davis-Poynter, N., 2007. A point mutation in a herpesvirus polymerase determines neuropathogenicity. PLos Pathog. 3, 1583–1592.
Groth, A.C., Calos, M.P., 2004. Phage integrases: biology and applications. J. Mol. Biol. 335, 667–678.
Hansen, K., Napier, I., Koen, M., Bradford, S., Messerle, M., Bell, E., Seshadri, L., Stokes, H.W., Birch, D., Whalley, J.M., 2006. In vitro transposon mutagenesis of an equine herpesvirus 1 genome cloned as a bacterial artificial chromosome. Arch. Virol. 151, 2389–2405.
Harty, R.N., Caughman, G.B., Holden, V.R., O'Callaghan, D.J., 1993. Characterization of the myristylated polypeptide encoded by the UL1 gene that is conserved in the genome of defective interfering particles of equine herpesvirus 1. J. Virol. 67, 4122–4132.
Hirt, B., 1967. Selective extraction of polyoma DNA from infected mouse cell cultures. J. Mol. Biol. 26, 365–369.
Ho, D.Y., Mocarski, E.S., 1988. Beta-galactosidase as a marker in the peripheral and neural tissues of the herpes simplex virus-infected mouse. Virology 167, 279–283.
Jackson, T.A., Osburn, B.I., Cordy, D.R., Kendrick, J.W., 1977. Equine herpesvirus 1 infection of horses: studies on the experimentally induced neurologic disease. Am. J. Vet. Res. 38, 709–719.

Jacobson, J.G., Martin, S.L., Coen, D.M., 1989. A conserved open reading frame that overlaps the herpes simplex virus thymidine kinase gene is important for viral growth in cell culture. J. Virol. 63, 1839–1843.
Kanda, T., Yajima, M., Ahsan, N., Tanaka, M., Takada, K., 2004. Production of high-titer Epstein–Barr virus recombinants derived from Akata cells by using a bacterial artificial chromosome system. J. Virol. 78, 7004–7015.
Kirisawa, R., Ohmori, H., Iwai, H., Kawakami, Y., 1993. The genomic diversity among equine herpesvirus-1 strains isolated in Japan. Arch. Virol. 129, 11–22.
Kohn, C.W., Fenner, W.R., 1987. Equine herpes myeloencephalopathy. Vet. Clin. North Am., Equine Pract. 3, 405–419.
Leist, T.P., Sandri-Goldin, R.M., Stevens, J.G., 1989. Latent infections in spinal ganglia with thymidine kinase-deficient herpes simplex virus. J. Virol. 63, 4976–4978.
Leutenegger, C.M., Madigan, J.E., Mapes, S., Thao, M., Estrada, M., Pusterla, N., 2008. Detection of EHV-1 neuropathogenic strains using real-time PCR in the neural tissue of horses with myeloencephalopathy. Vet. Rec. 162, 688–690.
Livak, K.J., Schmittgen, T.D., 2001. Analysis of relative gene expression data using real-time quantitative PCR and the $2^{-\Delta\Delta C_T}$ method. Methods 25, 402–408.
Matsumura, T., Sugiura, T., Imagawa, H., Fukunaga, Y., Kamada, M., 1992. Epizootiological aspects of type 1 and type 4 equine herpesvirus infections among horse populations. J. Vet. Med. Sci. 54, 207–211.
Matsumura, T., Kondo, T., Sugita, S., Damiani, A.M., O'Callaghan, D.J., Imagawa, H., 1998. An equine herpesvirus type 1 recombinant with a deletion in the gE and gI genes is avirulent in young horses. Virology 242, 68–79.
Meignier, B., Longnecker, R., Mavromara-Nazos, P., Sears, A.E., Roizman, B., 1988. Virulence and establishment of latency by genetically engineered deletion mutants of herpes simplex virus 1. Virology 162, 251–254.
Nash, H.A., 1990. Bending and supercoiling of DNA at the attachment site of bacteriophage lambda. Trends Biochem. Sci. 15, 222–227.
Nash, H.A., Robertson, C.A., 1981. Purification and properties of the *Escherichia coli* protein factor required for lambda integrative recombination. J. Biol. Chem. 256, 9246–9253.
Nugent, J., Birch-Machin, I., Smith, K.C., Mumford, J.A., Swann, Z., Newton, J.R., Bowden, R.J., Allen, G.P., Davis-Poynter, N., 2006. Analysis of equid herpesvirus 1 strain variation reveals a point mutation of the DNA polymerase strongly associated with neuropathogenic versus non neuropathogenic disease outbreaks. J. Virol. 80, 4047–4060.
Osterrieder, N., Neubauer, A., Brandmuller, C., Kaaden, O.R., O'Callaghan, D.J., 1996. The equine herpesvirus 1 IR6 protein influences virus growth at elevated temperature and is a major determinant of virulence. Virology 226, 243–251.
Pagamjav, O., Sakata, T., Matsumura, T., Yamaguchi, T., Fukushi, H., 2005. Natural recombinant between equine herpesviruses 1 and 4 in the ICP4 gene. Microbiol. Immunol. 49, 167–179.
Patsey, R.L., Bruist, M.F., 1995. Characterization of the interaction between the lambda intasome and *att*B. J. Mol. Biol. 252, 47–58.
Pearson, A., Coen, D.M., 2002. Identification, localization, and regulation of expression of the UL24 protein of herpes simplex virus type 1. J. Virol. 76, 10821–10828.
Rudolph, J., O'Callaghan, D.J., Osterrieder, N., 2002. Cloning of the genomes of equine herpesvirus type 1 (EHV-1) strains KyA and RacL11 as bacterial artificial chromosomes (BAC). J. Vet. Med. B Infect. Dis. Vet. Public Health 49, 31–36.
Sambrook, J., Fritsch, D.F., Maniatis, T., 1989. Molecular cloning: a laboratory manual, 2nd ed. Cold Spring Harbor Laboratory Press, Cold Spring Harbor, N.Y.
Sato, H., Pesnicak, L., Cohen, J.I., 2002. Varicella-zoster virus open reading frame 2 encodes a membrane phosphoprotein that is dispensable for viral replication and for establishment of latency. J. Virol. 76, 3575–3578.
Sears, A.E., Meignier, B., Roizman, B., 1985. Establishment of latency in mice by herpes simplex virus 1 recombinants that carry insertions affecting regulation of the thymidine kinase gene. J. Virol. 55, 410–416.
Shi, J., Biek, D.P., 1995. A versatile low-copy-number cloning vector derived from plasmid F. Gene 164, 55–58.
Smith, G.A., Enquist, L.W., 1999. Construction and transposon mutagenesis in *Escherichia coli* of a full-length infectious clone of pseudorabies virus, an alphaherpesvirus. J. Virol. 73, 6405–6414.
Smith, G.A., Enquist, L.W., 2000. A self-recombining bacterial artificial chromosome and its application for analysis of herpesvirus pathogenesis. Proc. Natl. Acad. Sci. U. S. A. 97, 4873–4878.
Smith, P.M., Kahan, S.M., Rorex, C.B., von Einem, J., Osterrieder, N., O'Callaghan, D.J., 2005. Expression of the full-length form of gp2 of equine herpesvirus 1 (EHV-1) completely restores respiratory virulence to the attenuated EHV-1 strain KyA in CBA mice. J. Virol. 79, 5105–5115.
Smith, K.L., Allen, G.P., Branscum, A.J., CooK, R.F., Vickers, M.L., Timoney, P.J., Balasuriya, U.B.R., 2010. The increased prevalence of neuropathogenic strains of EHV-1 in equine abortions. Vet. Microbiol. 141, 5–11.
Subak-Sharpe, J.H., Dargan, D.J., 1998. HSV molecular biology: general aspects of herpes simplex virus molecular biology. Virus Genes 16, 239–251.
Tanaka, M., Kagawa, H., Yamanashi, Y., Sata, T., Kawaguchi, Y., 2003. Construction of an excisable bacterial artificial chromosome containing a full-length infectious clone of herpes simplex virus type 1: viruses reconstituted from the clone exhibit wild-type properties in vitro and in vivo. J. Virol. 77, 1382–1391.
Telford, E.A., Watson, M.S., McBride, K., Davison, A.J., 1992. The DNA sequence of equine herpesvirus-1. Virology 189, 304–316.
Thomson, J.G., Rucker III, E.B., Piedrahita, J.A., 2003. Mutational analysis of loxP sites for efficient Cre-mediated insertion into genomic DNA. Genesis 36, 162–167.
Visalli, R.J., Brandt, C.R., 2002. Mutation of the herpes simplex virus 1 KOS UL45 gene reveals dose dependent effects on central nervous system growth. Arch. Virol. 147, 519–532.
Vissani, M.A., Becerra, M.L., Olguin Perglione, C., Tordoya, M.S., Barrandeguy, M., 2009. Neuropathogenic and non-neuropathogenic genotypes of eqiud Herpesvirus type1 in Argentina. Vet. Microbiol. 139, 361–364.
Wagner, M., Jonjic, S., Koszinowski, U.H., Messerle, M., 1999. Systematic excision of vector sequences from the BAC-cloned herpesvirus genome during virus reconstitution. J. Virol. 73, 7056–7060.
Ward, P.L., Roizman, B., 1994. Herpes simplex genes: the blueprint of a successful human pathogen. Trends Genet. 10, 267–274.
Whalley, J.M., Robertson, G.R., Davison, A.J., 1981. Analysis of the genome of equine herpesvirus type 1: arrangement of cleavage sites for restriction endonucleases EcoRI, BglII and BamHI. J. Gen. Virol. 57, 307–323.
Whitbeck, J.C., Lawrence, W.C., Bello, L.J., 1994. Characterization of the bovine herpes virus 1homolog of the herpes simplex virus 1 UL24 open reading frame. Virology 200, 263–270.
Yamada, S., Matsumura, T., Tsujimura, K., Yamaguchi, T., Ohya, K., Fukushi, H., 2008. Comparison of the growth kinetics of neuropathogenic and nonneuropathogenic equid herpesvirus type 1 (EHV-1) strains in cultured murine neuronal cells and the relevance of the D/N752 coding change in the DNA polymerase gene (ORF30). J. Vet. Med. Sci. 70, 505–511.
Yu, D., Smith, G.A., Enquist, L.W., Shenk, T., 2002. Construction of a self-excisable bacterial artificial chromosome containing the human cytomegalovirus genome and mutagenesis of the diploid TRL/IRL13 gene. J. Virol. 76, 2316–2328.
Zhang, Z., Rowe, J., Wang, W., Sommer, M., Arvin, A., Moffat, J., Zhu, H., 2007. Genetic analysis of varicella-zoster virus ORF0 to ORF4 by use of a novel luciferase bacterial artificial chromosome system. J. Virol. 81, 9024–9933.

Virus Genes (2010) 41:231–235
DOI 10.1007/s11262-010-0509-0

A novel genotype of beak and feather disease virus in budgerigars (*Melopsittacus undulatus*)

Hirohito Ogawa · Hiroshi Katoh · Naoko Sanada · Yasuyuki Sanada · Kenji Ohya · Tsuyoshi Yamaguchi · Hideto Fukushi

Received: 5 February 2010 / Accepted: 19 June 2010 / Published online: 25 July 2010

Abstract Beak and feather disease virus (BFDV) is a causative agent for psittacine beak and feather disease (PBFD), which shows a characteristic feather disorder in psittacine birds. Nineteen budgerigars, which were clinically suspected to have PBFD, were examined by two polymerase chain reactions (PCR), which target each of open reading frames (ORFs) V1 and C1. All of the 19 samples were detected BFDV by the PCR targeting ORF C1, whereas only two of them were detected by the PCR targeting ORF V1. It was assumed that BFDV derived from budgerigar (budgerigar BFDV) has two genotypes, which are tentatively classified as budgerigar BFDV genotype 1 and genotype 2 by the PCR amplification patterns. Whole genome sequences of six budgerigar BFDVs were determined to reveal the existence of two genotypes. In the phylogenic analysis, six budgerigar BFDV sequences formed a unique group branched from the other 23 published BFDV sequences. The budgerigar BFDV genotype 1 and genotype 2 were also segregated each other, and budgerigar BFDV genotype 2 was particularly distantly related with the other BFDVs. These results suggest budgerigar BFDV is a unique in the known BFDVs and is divided into two genotypes.

Keywords Psittacine beak and feather disease · PBFD · Beak and feather disease virus · Circovirus · Budgerigar

Electronic supplementary material The online version of this article (doi:10.1007/s11262-010-0509-0) contains supplementary material, which is available to authorized users.

H. Ogawa · H. Katoh · H. Fukushi
Department of Applied Veterinary Sciences, United Graduate School of Veterinary Sciences, Gifu University, 1-1 Yanagido, Gifu, Gifu 501-1193, Japan

N. Sanada · Y. Sanada
Bird's Hospital-BIRD HOUSE, 3-20-2 Akehara, Kashiwa, Chiba 277-0843, Japan

K. Ohya · H. Fukushi (✉)
Laboratory of Veterinary Microbiology and Infectious Diseases, Faculty of Applied Biological Sciences, Gifu University, 1-1 Yanagido, Gifu, Gifu 501-1193, Japan
e-mail: hfukushi@gifu-u.ac.jp

T. Yamaguchi
The Avian Zoonosis Research Center, Faculty of Agriculture, Tottori University, 4-101 Yanagido, Koyama Minami, Tottori 680-8550, Japan

Present Address:
H. Ogawa
Hokkaido University Research Center for Zoonosis Control, Kita-20, Nishi-10, Kita-ku, Sapporo 001-0020, Japan

Psittacine beak and feather disease (PBFD) is a specific disease in psittacine birds caused by beak and feather disease virus (BFDV), a member of genus *Circovirus* [1]. Clinical form of PBFD included chronic, progressive loss of feathers and, in some species, deformities of the beak and claws [2]. Acute-form, which shows signs of septicemia accompanied by pneumonia, enteritis, rapid weight loss, and death, has also been described [2]. BFDV carries a single-stranded circular DNA with a complete genome size of approximately 2.0 kb. The genome contains two major open reading frames (ORFs), encoding the replication-associated protein (V1), and the capsid protein (C1). Another ORF (ORF V2) has been also described, but it is unclear what role the transcriptional product of this ORF may play in the cycle of the virus [1].

PBFD has since been reported to affect more than 60 psittacine species; it is highly probable that all psittacine

bird species are susceptible [3]. So far, phylogenetic analysis of BFDV has revealed an apparent genotypic association with specific psittacine species [4, 5]. The level of genetic diversity has been reported to be similar among several countries such as Australia, New Zealand, and South Africa [5–7].

In the present study, 19 BFDV isolates derived from budgerigars (*Melopsittacus undulatus*) showing PBFD were detected by polymerase chain reactions (PCR), and of which six isolates were determined whole genome sequence. It was shown that 19 BFDV isolates in this study separated into two lineages, in addition, one was unique lineage to be reported previously.

Twenty samples including 13 feathers, 4 livers, and 3 bloods from 19 budgerigars in Japan suspected to be PBFD were examined in this study (Table 1). DNA was extracted from the blood or feathers with a SepaGene nucleic acid extraction kit (Sanko Junyaku Co., Japan) as described previously [8] and stored at −30°C until use. PCR was carried out using two sets of primer, Primer2/Primer4 (Ypelaar's PCR) and PBFDdupF/PBFDdupR (Ogawa's PCR) targeting BFDV genomic DNA previously described [8, 9]. As result of PCR, BFDV genomic DNA was detected in all 19 samples using primer set of PBFDdupF and PBFDdupR, whereas BFDV genomic DNA was amplified in only two samples using Primer2 and Primer4 (Table 1). These isolates were tentatively classified as budgerigar BFDV genotype 1, which was detectable by Ypelaar's PCR, and genotype 2, which was not detectable.

Next, we performed whole genome sequence analysis of these BFDV isolates, 4 and 2, respectively, were from acute-form and chronic-form, to determine their genetic characteristics. Whole genome sequences of six budgerigar BFDVs, of which 2 (MU-JP1P and MU-JP2P) and 4 (MU-JP3P to MU-JP6P) were genotype 1 and 2, were determined. Four fragments covering the whole genome were amplified by PCR using four primers sets for each genotype (Supplementary Table S1). PCR products were cloned and sequenced as described previously [8]. The obtained sequences were edited using Genetyx-Mac version 13 (Genetyx Co., Japan) and Genetyx-Mac/ATSQ version 4.2.4 (Genetyx Co.). The sequences of six

Table 1 Birds used in this study and genotypes of the budgerigar BFDV

Budgerigar	Age[a]	Clinical signs[b]	Clinical forms	Specimen	PCR results		Genotype	BFDVcode	Accession no.[c]
					Ogawa [8]	Ypelaar [9]			
Complete genome sequences determined in the present study									
Budgerigar1	42 d	Acute death	Acute	Liver	+	+	1	MU-JP1P	AB277746
Budgerigar2	2 y 6 m	Feather disorder	Chronic	Feather	+	+	1	MU-JP2P	AB277747
Budgerigar3	3 m	Acute death	Acute	Liver	+	−	2	MU-JP3P	AB277748
Budgerigar4	1 m	Acute death	Acute	Liver	+	−	2	MU-JP4P	AB277749
Budgerigar5	40 d	Acute death	Acute	Liver	+	−	2	MU-JP5P	AB277750
Budgerigar6	3 y	Feather disorder	Chronic	Feather	+	−	2	MU-JP6P	AB277751
Tested by PCR only and not sequenced in the present study									
Budgerigar7	45 d	Feather disorder	Chronic	Feather	+	−	2	MU-JP7P	
Budgerigar8	6 m	Feather disorder	Chronic	Feather	+	−	2	MU-JP8P	
Budgerigar9	4 m	Feather disorder	Chronic	Blood	+	−	2	MU-JP9P	
Budgerigar10	3 y	Feather disorder	Chronic	Feather	+	−	2	MU-JP10P	
Budgerigar11	1 y	Feather disorder	Chronic	Feather	+	−	2	MU-JP11P	
Budgerigar12	2 y	Feather disorder	Chronic	Blood	+	−	2	MU-JP12P	
Budgerigar13	2 m	Feather disorder	Chronic	B&F[d]	+	−	2	MU-JP13P	
Budgerigar14	1 y	Feather disorder	Chronic	Feather	+	−	2	MU-JP14P	
Budgerigar15	9 m	Feather disorder	Chronic	Feather	+	−	2	MU-JP15P	
Budgerigar16	2 y	Feather disorder	Chronic	Feather	+	−	2	MU-JP16P	
Budgerigar17	2 y 6 m	Feather disorder	Chronic	Feather	+	−	2	MU-JP17P	
Budgerigar18	5 y	Feather disorder	Chronic	Feather	+	−	2	MU-JP18P	
Budgerigar19	1 y 5 m	Feather disorder	Chronic	Feather	+	−	2	MU-JP19P	

[a] d, m, and y indicate days, month(s), and year(s), respectively

[b] Budgerigars affected with feather disorder are all alive

[c] Sequence of BFDV isolates derived from budgerigar7 to 19 is not determined

[d] B&F indicates blood and feather

budgerigar BFDV isolates have been submitted to GenBank and have been given accession numbers AB277746–AB277751. The genome sizes ranged from 1996 to 2004 nt (MU-JP1P, 1996 nt; MU-JP2P, 1996 nt; MU-JP3P, 2001 nt; MU-JP4P, 2004 nt; MU-JP5P, 2004 nt, and MU-JP6P, 2002 nt) (Supplementary Table S2). The identities of whole genome sequences of budgerigar BFDV genotype 1 and genotype 2 compared with the 23 published BFDV isolates shown in supplementary Table S3 from 87 to 92% and from 83 to 92%, respectively. Budgerigar BFDV genotype 1 whole genome sequences were from 85 to 88% identical to genotype 2 sequences. The identities of deduced amino acid sequences of budgerigar BFDV genotype 1 and genotype 2 ORF V1 compared to 23 published BFDVs varied from 90 to 99% and from 87 to 93%, respectively. Those of genotype 1 and genotype 2 ORF C1 varied from 75 to 91% and from 74 to 85%, respectively. The deduced amino acid sequences of ORF V1 and C1 of budgerigar BFDV genotype 1 were from 91 to 94% and from 84 to 88% identical to those of genotype 2, respectively.

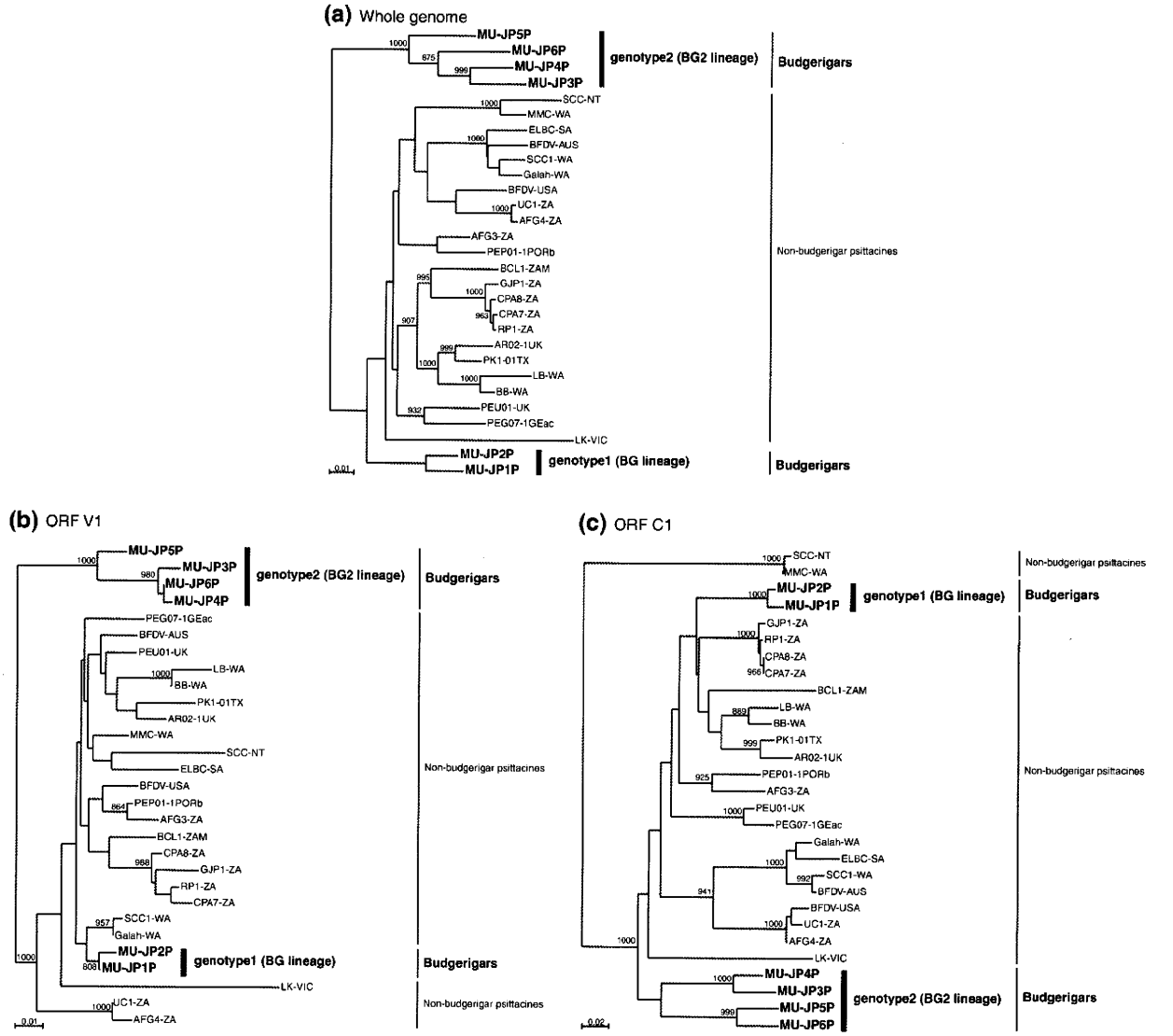

Fig. 1 Neighbor-joining tree of **a** complete genome sequence, amino acid sequences of **b** ORF V1 and **c** C1 of six budgerigar BFDVs and 23 BFDVs [1, 4–6]. The bootstrap values of each node were calculated using 1,000 replications. *Bold fonts* indicate budgerigar BFDV from the present study. Genbank accession numbers we used are AB277746–AB277751 in six budgerigar BFDV isolates, and AF311295–AF311302, AF080560, AF071878, AY521234–AY521238, AY450434, AY450436–AY450439 and AY450441–AY450443 in 23 non-budgerigar BFDV isolates, respectively. **a** Six budgerigar BFDV genome sequences formed different branches from 23 BFDVs, and budgerigar BFDV genotype 1 and genotype 2 were also in independent clusters. **b** and **c** Budgerigar BFDV genotype 1 was closely related to 23 BFDVs in the both trees, whereas genotype 2 was distantly related to them